

Optical Investigation of Suspended Single Wall Carbon Nanotubes

by

Dávid Lakatos

A thesis submitted in partial fulfillment for the
degree of Bachelor of Science

in the

[Budapest University of Technology and Economics](#)

Department of Broadband Infocommunications and Electromagnetic Theory

Group of Electromagnetic Theory

and

[Delft University of Technology](#)

Department of Nanosciences

Quantum Transport Group

December 2009

Declaration of Authorship

I, David Lakatos, declare that this thesis titled, ‘Optical investigation of suspended carbon nanotubes’ and the work presented in it are my own. I confirm that:

- This work was done wholly or mainly while in candidature for a research degree at this University.
- Where any part of this thesis has previously been submitted for a degree or any other qualification at this University or any other institution, this has been clearly stated.
- Where I have quoted from the work of others, the source is always given. With the exception of such quotations, this thesis is entirely my own work.
- I have acknowledged all main sources of help.

Signed:

Date:

Contents

Declaration of Authorship	i
List of Figures	iii
Abbreviations	iv
1 Introduction	1
2 Background	3
2.1 Single wall carbon nanotubes	3
2.1.1 Atomic structure	3
2.1.2 Electronic structure	6
2.1.3 Optical properties	10
2.2 Synthesis	12
2.2.1 Sample preparation methods	12
2.2.2 Samples used in the experiments	13
3 Experimental design	16
3.1 Equipment	16
3.1.1 Confocal microscope setup	16
3.1.2 Spectrometer	18
3.1.3 Lasers	21
3.1.4 Motors	21
3.1.5 Power meter	21
3.2 Description of the measurement procedures	22
3.3 PLE mapping automatization	22
3.3.1 Manual search and sample mapping	23
4 Results	25
4.1 Locating SWCNTs	25
4.2 The aging effect of SWCNTs	29
4.3 Sample mapping	31
4.4 PLE mapping	31
5 Conclusion and Outlook	35
5.1 Conclusion and outlook	35

A Program codes	37
A.1 RT_Setup.m	37
A.2 getbeam.m	58
A.3 plemap.m	64
B Graphical User Interfaces	77
C Table for assigning chiral indices	81
Bibliography	83
Acknowledgements	86

List of Figures

2.1	The three types of tubes: zigzag, armchair and chiral.	5
2.2	The chiral and translation vectors of CNTs	5
2.3	Unit vectors in real (a) and reciprocal space (b)	7
2.4	The periodic boundary condition using the ZF approximation	8
2.5	Reciprocal lattice of graphene with energy contour plot of the bonding band and allowed k-lines for a metallic (5,5) and a semiconducting (10,0) nanotube	9
2.6	Electronic band structure and Density of states for a (4,2) nanotube	9
2.8	Density of states with bandgap renormalization	11
2.7	E_{22} (excitation) and E_{11} (emission) energies	11
2.9	Pillar spacing dependence of bridging probability of suspended SWCNTs grown on a square-lattice pillar array.	13
2.10	Schematics of the samples from Waseda University, Tokyo	14
2.11	SEM images of the samples (Trenches and pillars region)	14
2.12	SEM image of the sample from NRC	14
3.1	a) Schematics of the home built confocal microscope setup. b) Picture of the confocal microscope setup mounted on a dedicated optical table.	17
3.2	Schematic of the monochromator	18
3.3	Flowchart of the PLE automatization	23
4.1	Measured photoluminescence of a single SWCNT	26
4.2	Photoluminescence spectrum of a nanotube with a Lorentzian-fit	27
4.3	Setup modification in order to increase the beam size	28
4.4	Beam diameter measurement from the CCD image	29
4.5	Aging effect of nanotubes	30
4.6	Aging effect of nanotubes II.	30
4.7	Mapped samples with possible nanotubes	32
4.8	PLE map of a (11, 6) individual nanotube	33
B.1	GUI for the sample mapping automatization and stage control	78
B.2	GUI for the beam area calculation	79
B.3	GUI for the PLE mapping automatization	80
C.1	Table for assigning chiral indices to nanotubes based on their E_{11} and E_{22} energies	82

Abbreviations

BZ	B rillouin Z one
CCD	C harge- C oupled D evice
CNT	C arbon- N anotube
CVD	C hemical V apor D eposition
DLL	D ynamic L ink L ibrary
GUI	G raphical U ser I nterface
IR	I nfra r ed
InGaAs	I ndium G allium A rsenide
MWCNT	M ulti-walled C arbon N anotube
NA	N umerical A perture
NIR	N ear I nfrared
NRC	N ational R esearch C ouncil (Canada)
PL	P hotoluminescence
PLE	P hotoluminescence E xcitation
SEM	S canning E lectron M icroscope
SWCNT	S ingle W all C arbon N anotube
TB	T ight- B inding
USB	U niversal S erial B us
VHS	V an H ove S ingularity
ZF	Z one- F olding

Chapter 1

Introduction

The era of microelectronics is approaching its end, because scaling down electronic device dimensions is slowly reaching fundamental physical limits. In order to continue the envisioned path of Gordon E. Moore - who predicted that the computational power of semiconductor electronics will double, roughly every two years - a new technology has to be implemented. Nanotechnology provides a new perspective in fabrication, in comparison with the usual top-down scheme used in microelectronics, with the so-called bottom-up technique where nanostructures are assembled at nearly atomic levels. Working according to this philosophy, device dimensions can be scaled down to individual atoms.

The phenomena occurring at the nanometer scale cannot be described by classical physics anymore, but only by quantum mechanics. When the dimensions of objects shrink down to the nanometer scale, new properties emerge. One well-known example for this is given by graphite. Graphite (a stacking of two-dimensional, sp^2 -bonded carbon layers) is known as a mechanically soft material, which is used in pencil leads. Now, if one imagines isolating a small sheet of a graphite monolayer (graphene) and roll it into a cylinder with a nanometric diameter, one will obtain a nano-object with amazing mechanical (tensile strength 80 times higher than high strength steel), thermal (better than copper) and electronic properties (completely described by tube geometry). Such objects called carbon nanotubes (CNT) have been discovered in 1991 by Sumio Iijima at NEC [1] and since then have led to an explosion of research activities in many labs worldwide. Furthermore, recent studies showed very promising optical properties which allow new applications and research in nanotube-based optoelectronics [2]. Their importance even grew in the recent past, since in the field of quantum information processing, carbon

nanotubes are potential candidates that are able to naturally link solid state qubits used for information processing (such as single spins), with flying qubits used to transmit quantum information (photons) [3, 4].

The goal of my thesis is to get familiarized with carbon nanotube physics and related experimental techniques. Here the focus was put on the optical properties of single wall carbon nanotubes (SWCNT). I studied the photoluminescence (PL) of suspended carbon nanotubes on diverse samples. I implemented a system to facilitate the investigation of the photoluminescence excitation (PLE) mapping, which helped identifying the structure of the investigated nanotubes. Furthermore, I have come across an effect called bleaching, which corresponds to the decay of the PL signal. Based on the available literature, we addressed reasons behind this observation.

Chapter 2

Background

Carbon nanotubes discovered in 1991 by S. Iijima [1], are important to scientists and engineers, because of their outstanding physical properties [5]. SWCNTs can be regarded as a sheet of graphene (one layer of graphite is called graphene) rolled into a cylinder. Among several nanostructures, carbon nanotubes have the smallest aspect ratio: in diameter they are only a few nanometers wide, but their length is usually a couple of μm , although it is possible to grow tubes that are as long as several cm [6]. Thus they are a quasi one-dimensional system, where quantum effects play a dominant role. The electronic structure of SWCNTs, that can be derived from the one of graphene, are unique in the sense that they are completely determined by the tube geometry, resulting in semiconducting or metallic character [5]. Furthermore SWCNTs are unique in the sense that they have prominent thermal [7], mechanical [7], chemical [8], electronic [5, 9] and optical properties [2]. In the next sections, the electronic and optical properties will be described in details.

2.1 Single wall carbon nanotubes

2.1.1 Atomic structure

The atomic number of carbon is 6 and as a group 14 element, four electrons are available to form covalent chemical bonds. The orbital structure of carbon consists of two electrons occupying the inner 1s shell. The other four can be arranged in 3 different ways, in other words, they can have three different hybridizations:

- sp^3 (4 covalent σ bonds), e.g.: diamond
- sp^2 (3 covalent σ bonds and 1 Π -bond), e.g.: graphene
- sp^1 (2 covalent σ bonds and 2 Π -bond)

In graphene and SWCNTs we have a sp^2 hybridization. In graphene, the honeycomb lattice builds up from three in-plane covalent σ bonds and a fourth π -bond, which is delocalised. Since SWCNTs are made up of graphene sheets rolled up into a cylinder, the three σ bonds are generally slightly out of plane due to the curvature and the π -bond gets delocalized along the tube walls. These σ bonds provide SWCNTs high mechanical strength along the tube axis - it has been measured that the Young's modulus for SWCNTs can be 80-times higher than that of high strength steel [10].

Now the nomenclature of nanotubes will be introduced. On Fig. 2.2, the honeycomb lattice structure of graphene is shown. Starting from one gridpoint (one C atom) using the linear combination of the basis vectors \vec{a}_1 and \vec{a}_2 , we can build up one of the two sublattices of graphene. By repeating this process, starting from one of the neighboring atoms of the initial starting point, the complementary sublattice can be constructed. The chiral vector of a CNT is the circumferential vector along which the sheet of graphene is rolled up. We can express this chiral vector as a linear combination of the basis vectors, \vec{a}_1 and \vec{a}_2 :

$$\vec{C} = n\vec{a}_1 + m\vec{a}_2, \quad \mathbf{n}, \mathbf{m} \in \mathbb{N} \quad (2.1)$$

Many properties of SWCNTs can be derived from the chiral vector, therefore a comfortable notation is used to describe them: from the equation above, the two integers n and m , which are called chiral indices are expressed in brackets, such as (n, m) .

Depending on the chiral indices one can separate SWCNTs into three main groups (see Fig. 2.1):

- if m or $n = 0$, the nanotube is called **zigzag**
- if $n = m$, the nanotube is called **armchair**
- if $n \neq m$ the nanotube is called **chiral**

In real space the other important geometrical parameter of a CNT is the translational vector, which represents the smallest vector along the tube axis, which connects two equivalent lattice

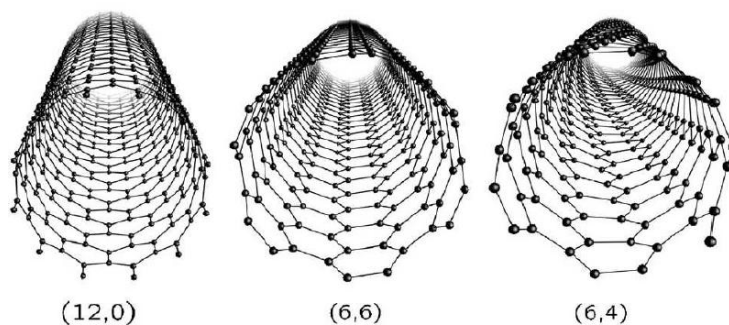


FIGURE 2.1: The three types of tubes: zigzag, armchair and chiral.

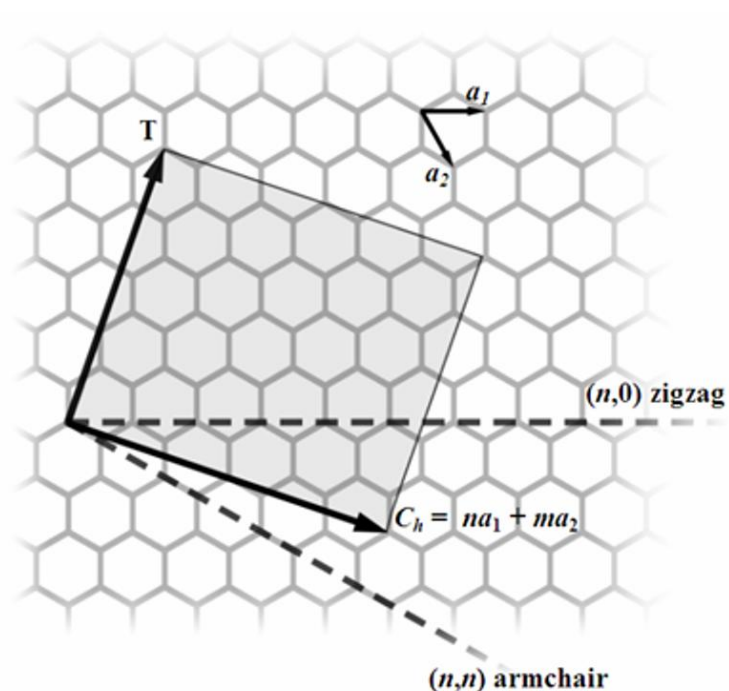


FIGURE 2.2: The chiral and translation vectors of CNTs

points. The translational vector is perpendicular to the chiral vector, and can be expressed again only with the chiral indices:

$$\mathbf{T} = t_1 \mathbf{a}_1 + t_2 \mathbf{a}_2, \quad t_1 = \frac{2m+n}{N_R}, \quad t_2 = -\frac{2m+n}{N_R} \quad (2.2)$$

where N_R is the greatest common divisor of $(2m+n)$ and $(2n+m)$.

The diameter of the tube can be expressed with only the chiral indices:

$$d_t = \frac{|C_h|}{\pi} = \frac{a}{\pi} \sqrt{n^2 + nm + m^2} \quad (2.3)$$

where a represents the lattice constant of the honeycomb lattice ($a = \sqrt{3}a_{cc} = |\vec{a}_1| = |\vec{a}_2|$, where a_{cc} is the the bond length with $a_{cc} \approx 1.42\text{\AA}$).

2.1.2 Electronic structure

As mentioned above, the electronic structure of a SWCNT can be derived from that of graphene. The unit cell of graphene is a rhombus that contains two carbon atoms as shown on Fig. 2.3 (a), in the dashed area. These two atoms belong to the two complementary sublattices that yield together the honeycomb lattice of graphene (A for sublattice A, B for sublattice B).

In the reciprocal space the corresponding BZ of graphene is similarly a honeycomb cell, as outlined red in Fig. 2.3 (b). The reciprocal lattice vectors are obtained from the condition $\vec{a}_i \cdot \vec{b}_j = 2\pi\delta_{ij}$:

$$\vec{b}_1 = \left(\frac{2\pi}{\sqrt{3}a}, \frac{2\pi}{a}\right) \quad \text{and} \quad \vec{b}_2 = \left(\frac{2\pi}{\sqrt{3}a}, -\frac{2\pi}{a}\right) \quad (2.4)$$

Using a tight-binding (TB) model, we can calculate the electronic structure of an infinite graphene sheet. The TB model is an approximation that only considers the interactions between neighboring atoms as perturbation and ignores the electron-electron interactions [11]. The calculations yield two wavefunctions, corresponding to the two complementary sublattices of electrons. From these wavefunctions the dispersion relation of graphene can be calculated [8] as later shown on Fig. 2.6 a.).

The electronic band structure is usually referenced in three high symmetry points, labeled on Fig. 2.3 with Γ , K and M (see Fig. 2.3 and 2.6 a.).

According to [12], the unit cell of SWCNTs, spanned by the translational and chiral vectors, contains

$$N = \frac{2(m^2 + mn + n^2)}{d_R} \quad (2.5)$$

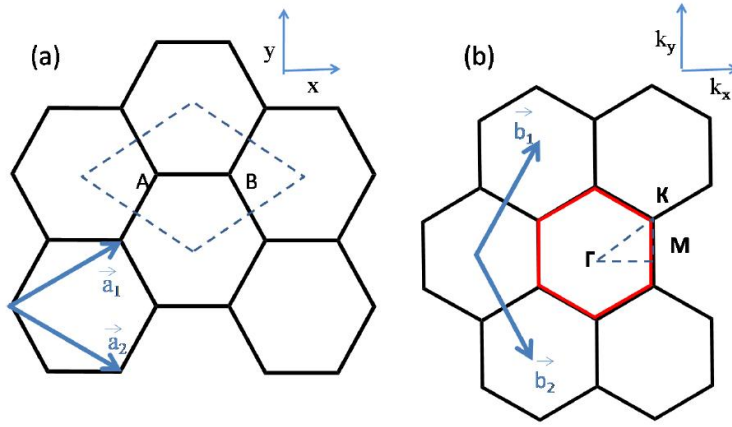


FIGURE 2.3: Unit vectors in real (a) and reciprocal space (b), [Adapted from "Unusual Properties and Structure of Carbon Nanotubes" [12]]

atoms which is much larger than that of graphene with only a two atom rhombus. This fact is important, because the number of electrons in the unit cell corresponds to the number of bands in the BZ, respectively.

In order to calculate the electronic structure of a SWCNT the zone-folding (ZF) approximation is used [11]. ZF approximation utilizes the fact that a rolled up sheet of graphene has periodic boundary conditions along the circumference of a SWCNT, thus the allowed wave vectors in direction perpendicular to the tube axis are quantized.

The periodic boundary condition is illustrated on Fig. 2.4. Due to the tubular structure of the SWCNT the wavefunctions at points P_1 and P_2 (with exactly one \vec{C} between them) have to satisfy the following condition:

$$\begin{aligned}
 \Psi(\vec{x}) &= \Psi(\vec{x} + \vec{C}) \\
 \implies e^{i\vec{k}\cdot\vec{x}} &= e^{i\vec{k}\cdot(\vec{x} + \vec{C})} \\
 &\implies e^{i\vec{k}\cdot\vec{C}} = 1 \\
 &\implies \vec{k} \cdot \vec{C} = 2\pi n
 \end{aligned} \tag{2.6}$$

Note: the second equation is a corollary of the Bloch-theorem. Plotting these allowed vectors for a given SWCNT onto the BZ of graphene generates a series of parallel and equidistant lines. The distance between lines can be calculated and is found to be $\Delta k = \frac{2}{d_t}$. The length, number

and orientation of these lines depend on the chiral indices (n,m) [12]. These parallel cutting lines decide to which group a nanotube belongs to. For example the parallel lines shown in Fig. 2.5 are examples of allowed k modes for a metallic $(5,5)$ armchair and a semiconducting $(10,0)$ zigzag, respectively. Note: the white and black plots in Fig. 2.5 are equipotential lines of the electronic structure of graphene shown in Fig. 2.6 a).

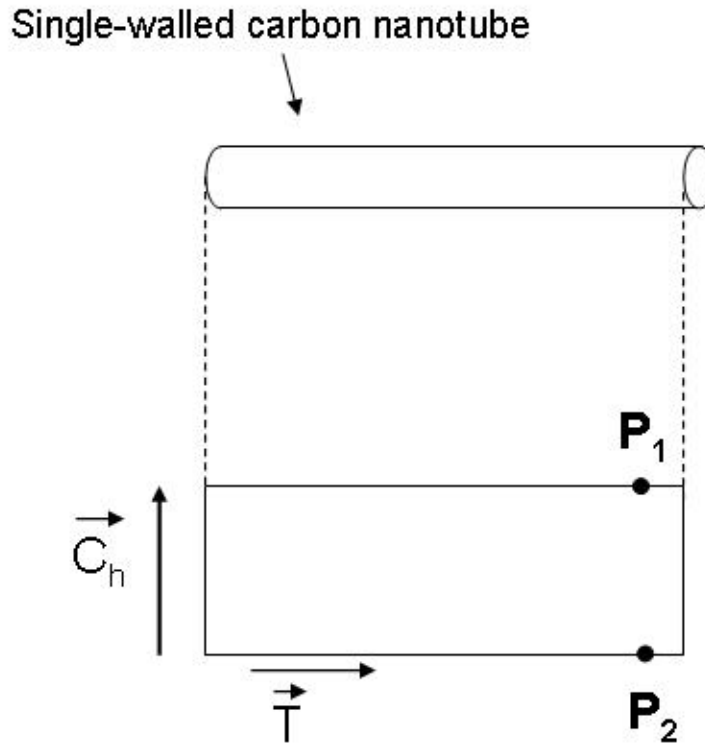


FIGURE 2.4: The periodic boundary condition using the ZF approximation

The basic idea behind the zone-folding approximation is that the electronic band structure of a specific nanotube is given by the superposition of the electronic energy bands along the corresponding allowed k lines as shown in Fig. 2.5, i.e. a pair of conduction and valence bands for each k line. Therefore the band structure in Fig. 2.6 b) correspond to the superposition of the line cuts in Fig. 2.6 a). If the K point is crossed by an allowed k line, the SWCNT is metallic, i.e the valence and the conduction band touch each other. It can be shown that a SWCNT is metallic if the condition $n - m = 3l$, with l an integer, is fulfilled.

When $n - m = 3 \cdot l \pm 1$, the allowed k vectors do not cross the K points, making the SWCNT semiconducting with a direct band gap. The band structure shown in Fig. 2.6 b) corresponds to the one of a $(4,2)$ semiconducting SWCNT. It can be calculated that a semiconducting SWCNT has a band gap of:

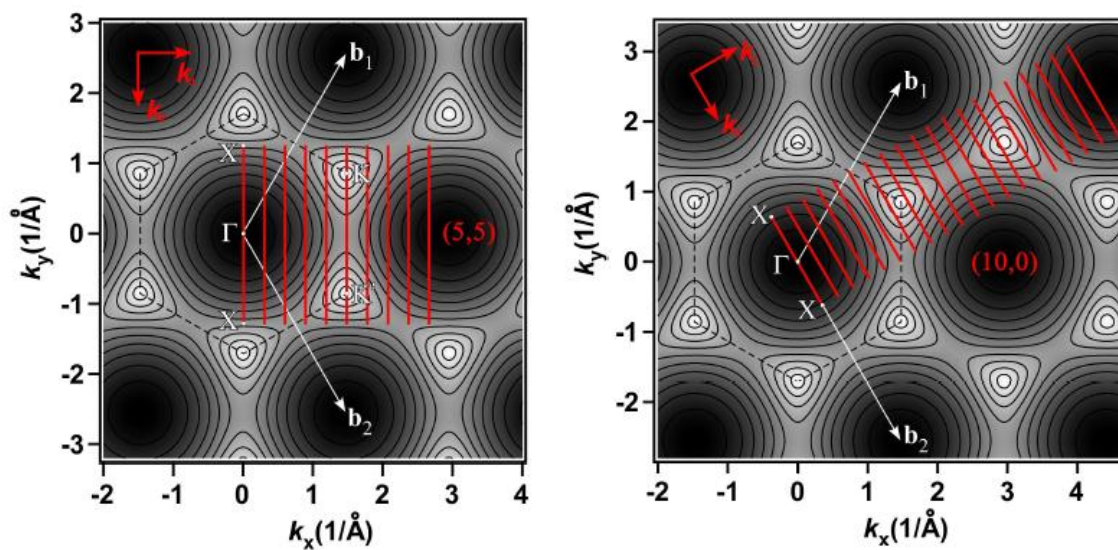


FIGURE 2.5: Reciprocal lattice of graphene with energy contour plot of the bonding band. The allowed k lines for SWCNTs arising from the quantization condition around the circumference: $C_h k = 2\pi q$ are drawn in red. k_{\parallel} and k_{\perp} are the unit vectors in directions of C_h and T , respectively. Left: metallic (5,5); Right: semiconducting (10,0) nanotubes

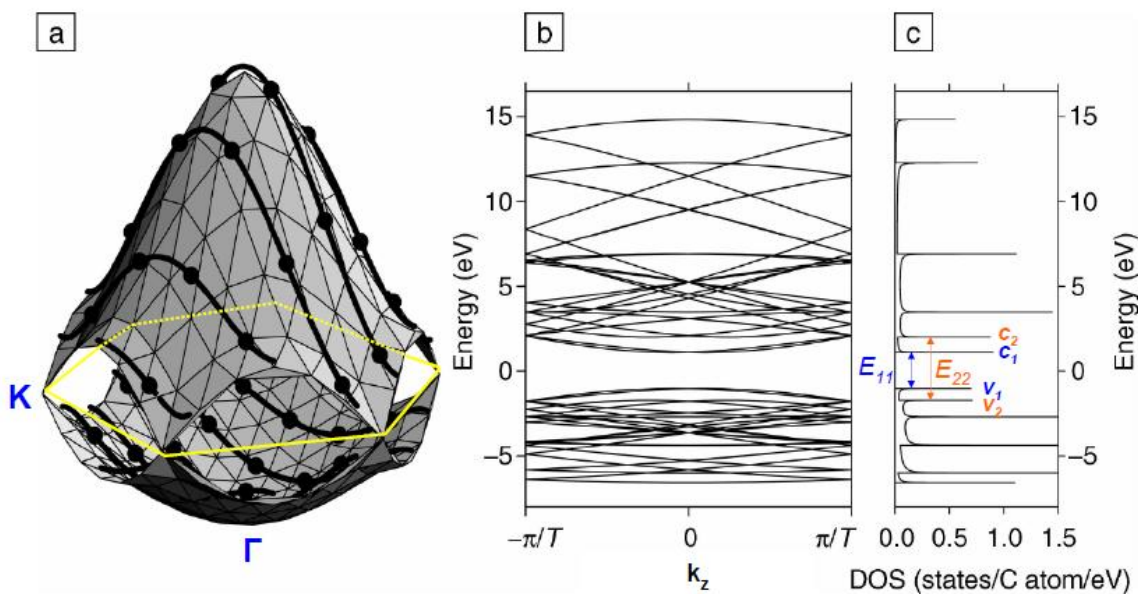


FIGURE 2.6: The dispersion relation (a), the electronic band structure (b) and the density of states (c) for a (4,2) carbon nanotube. The zero energy represents the Fermi level]

$$\Delta E_g = \frac{2a_{cc}}{d_t} \quad (2.7)$$

This $\frac{1}{d_t}$ dependence relies on the assumption of a linear dispersion cone around K-points in the BZ of graphene.

Due to its 1D character, the density of states (DOS) $\Delta N/\Delta E$ of SWCNTs is proportional to $(|\frac{\delta E(k)}{\delta k}|)^{-1}$ and diverges as $|E|/\sqrt{E^2 - (E_0)^2}$ close to band extrema E_0 , as can be seen in the right hand panels of Fig. 2.6 c). These singularities in the DOS are called Van Hove singularities (VHS) and are important to understand the optical properties of SWCNTs.

It is important to understand that in the TB calculations above, the Coulomb interactions are omitted and only proceed with the calculations for the neighboring atoms in the lattice.

2.1.3 Optical properties

Photoluminescence (PL) is a process in which a substance absorbs one or many photons and then re-radiates photons. In quantum mechanics, this can be described as an excitation to a higher energy state and then a return to a lower energy state accompanied by the emission of a photon.

Photoluminescence in semiconducting nanotubes, which are direct bandgap systems, was observed for the first time in 2002 and opened the way to carbon nanotube optics [13]. In this experiment, carbon nanotubes were wrapped in a solution in order to separate individual tubes from bundles. After studying the PL signal of SWCNTs wrapped in various surfactants, it became clear that the wrapping material influences the PL spectra. Later it has been shown also that experimental conditions, such as temperature and pH of the solution alter the measured spectra of SWCNTs as well [14–16].

In this work, we used suspended nanotubes that were grown between structures that separate them from the substrate material (as described in the following section). Since suspended SWCNTs do not contact substrates or any surrounding medium and have been shown to emit intense and sharp PL peaks [17], they are ideal systems for the investigation of the optical properties of individual tubes. A quantitative comparison between the PL spectra from suspended nanotubes

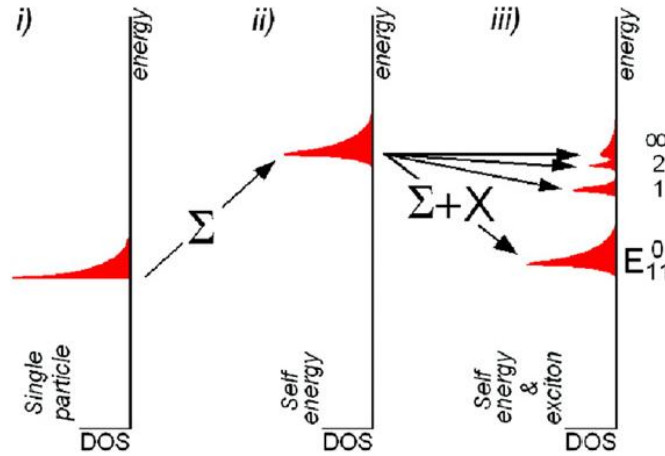


FIGURE 2.8: Density of states as suggested by i) TB approximation ii) TB approximation with Coulomb interaction iii) the normalized discrete excitonic states

and micelle-encapsulated nanotubes was reported by Jacques Lefebvre et al. and showed a red-shift of 28 meV in average for E_{11} and 16 meV for E_{22} for encapsulated nanotubes compared to air-suspended SWCNTs [18].

The absorption and emission energies are usually not the same in experiments. Nanotubes are excited with light polarized in the direction of the tube axis (antenna effect) in the E_{22} transition, and PL is measured from radiation in the E_{11} transition (Fig. 2.7). The E_{22}/E_{11} ratio from TB calculations is 2. However, experimental results yield a ratio around 1.8. This paradoxical observation is called the ratio-problem. This is due to the presence of excitonic states in the nanotube band gap.

An exciton consists of a photo-excited electron and hole bound to each other by a Coulomb interaction in a semiconducting material. In most bulk materials the binding energy is so low (magnitude of meV) that excitonic states can only be observed at very low temperatures. In the case of SWCNTs, because of their quasi one dimensionality, the confinement of particles is so high that the Coulomb interactions give rise to exciton binding energies of about 1/3 of the band gap [19], making the excitonic nature of SWCNTs observable at room temperature.

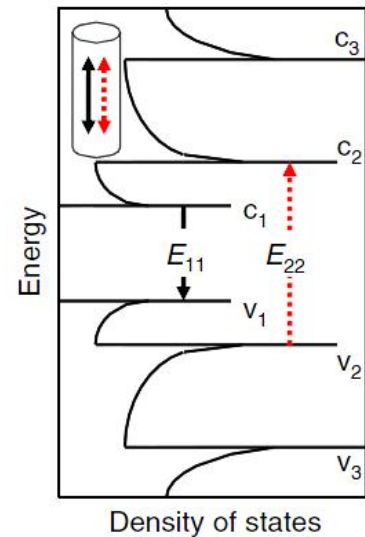


FIGURE 2.7: E_{22} (excitation) and E_{11} (emission) energies

A more detailed view of the excitonic effects occurring in semiconducting nanotubes is depicted in Fig. 2.8. The emission energies in SWCNTs are the result of two nearly equally important Coulomb interactions, the self-energy which increases the band gap (ii) in the single particle model (TB) (i) and the excitonic binding energy which decreases it (iii) with a series of discrete excitonic states below the self-energy corrected continuum.

2.2 Synthesis

2.2.1 Sample preparation methods

Carbon nanotubes can be synthesized by various methods with arc-discharge, laser-ablation and chemical vapor deposition (CVD) being the principal ones. The SWCNTs used in this work have been produced by CVD method. In CVD, a flowing hydrocarbon gas is decomposed at a growth temperature between 500 and 1000°C. The precipitation of carbon from the saturated phase in metal catalyst particles (generally Fe, Ni or Co) leads to the formation of a tubular carbon solid.

In the optical properties section it has been discussed that nanotubes lying on substrate material do not exhibit PL [17]. In the experiments I used suspended carbon nanotubes to avoid the environmental effect induced by the substrate material. The suspension of nanotubes can be done in multiple ways, but in my experiments I used mesa-structures where nanotubes are grown by CVD from catalytic particles lying on the mesa-structures. The mesa-structures used are trenches or pillars with different pitches.

The spacing between two mesa-structures (consecutive trenches, pillars) has influence on the tube bridging probability to a great extent. Fig. 2.9 shows the bridging probability (the percentage of pillar-pillar connections that have nanotubes growing between them) as a function of pillar-pillar distance. It can be seen that for increasing pillar-pillar distance, the number of connections decreases exponentially. Note: if the pillar-pillar distance approaches zero, the probability of bundled nanotubes rises dramatically. Bundles of nanotubes generally quench the PL and are therefore to avoid. It is preferable to have a larger distance between the pillars, thus a lower bridging probability, but less entanglement. For a more in-depth analysis of the synthesis of the synthesis of suspended tube samples, please refer to [20].

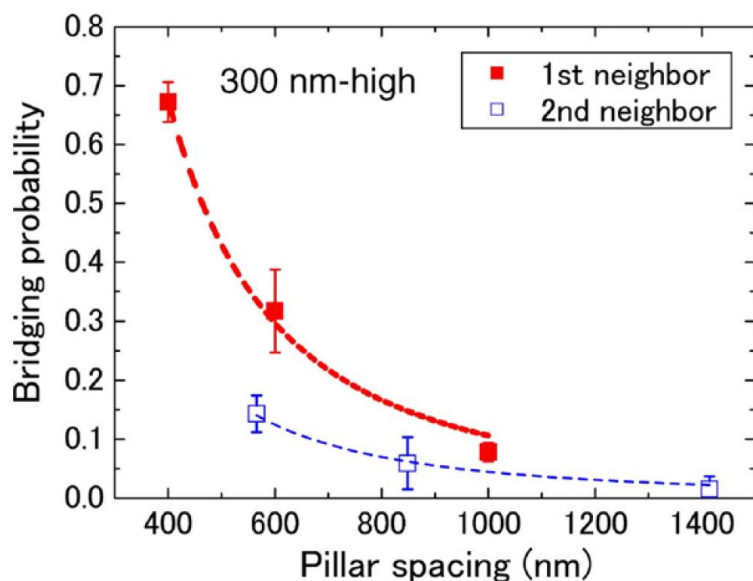


FIGURE 2.9: Pillar spacing dependence of bridging probability of suspended SWCNTs grown on a square-lattice pillar array.

While the growth techniques described yield a high amount of high-quality nanotubes, the formation mechanism of SWCNTs is still unknown. Previously the growth direction and speed was credited to the flow of gas on the sample, but a series of experiments done by at Tokyo University showed that SWCNT growth can occur even perpendicularly with respect to direction of the gas flow [21].

2.2.2 Samples used in the experiments

In our experiments the samples were provided from three research groups: from Waseda University, Tokyo; from NRC, Canada and from TU Delft. The fabrication method applied was CVD in all three cases. The pattern profile differed from sample to sample.

The samples provided by Prof. Y. Homma (Waseda University, Tokyo) have a Si substrate as base material and the SWCNT are grown on the surface with a CVD technique. The group used Co catalysts on their patterns to induce nanotube growth. Different patterns were defined with chemical etching. As Fig. 2.10 shows, the samples have 10 regions consisting of trenches (Fig. 2.11 a)), while the other consists of pillars (Fig. 2.11 b)).

It is important to note that one of the three samples provided by Waseda University has been investigated by SEM imaging (as seen on Fig. 2.11). It is known that high-energy electron irradiation on a nanotube causes structural damage due to a ballistic ejection of carbon atoms.

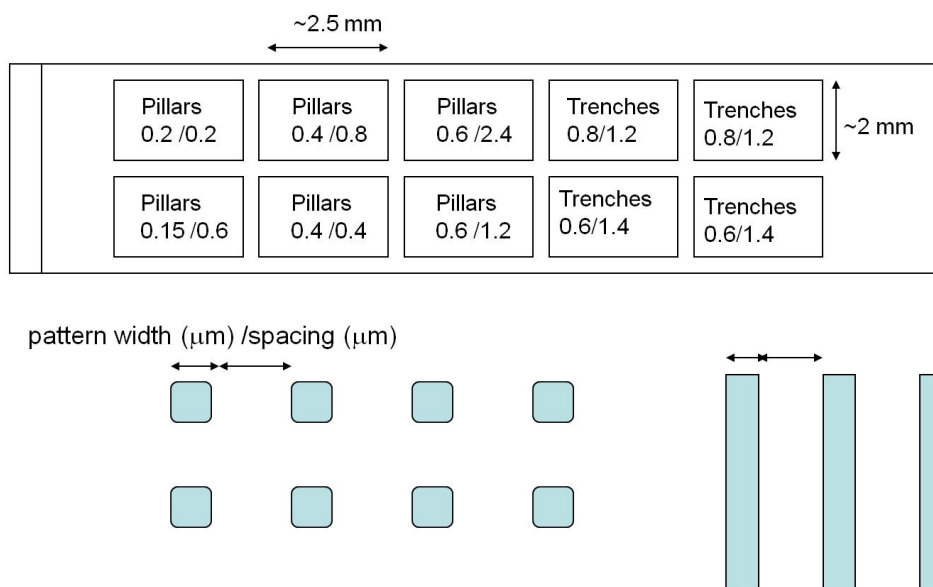


FIGURE 2.10: Schematics of the samples

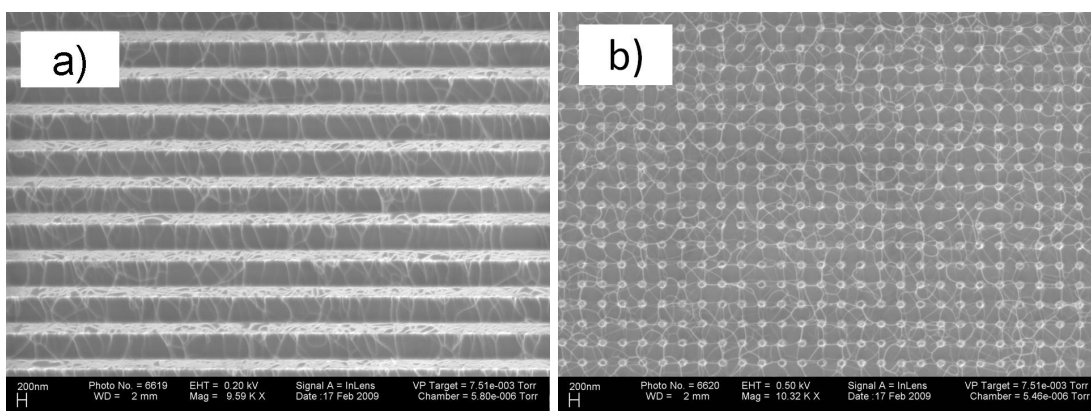


FIGURE 2.11: SEM images of the samples

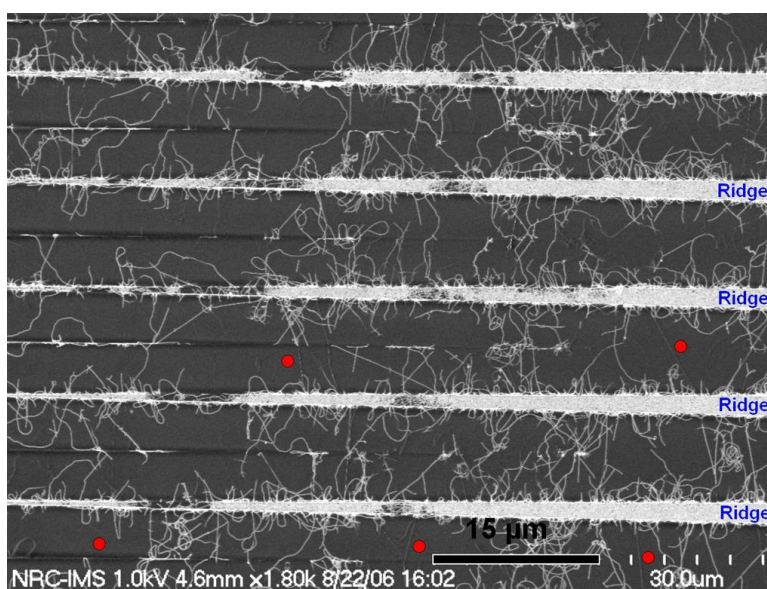


FIGURE 2.12: SEM image of the sample

Experimentally it has been shown that this effect leads to the decrease of the PL of nanotubes. However this phenomenon is paradoxical: since the threshold of ejection of carbon nanotubes is 86 keV, whereas SEM imaging bombards the sample only with 0.5-25keV electrons [22]. Interestingly it has been reported that these structural defect heal at room temperature, depending on the diameter of the nanotubes [23].

The samples from NRC are similar to the samples from Waseda University. They are made of trenches only, as shown on the SEM image on Fig. 2.12.

The last group of samples were designed and synthesized by the QT group of TU Delft. The patterns on the sample consists only of trenches, which are spaced periodically.

Chapter 3

Experimental design

3.1 Equipment

3.1.1 Confocal microscope setup

Suspended individual carbon nanotubes emit light in the NIR when excited in their E_{22} transitions. In order to study this effect we built a dedicated confocal microscope setup for near infrared optics, optimized for PL detection of nanotubes. The schematics as well as a picture (early stage) of the setup are shown in Figure 3.1 a) and b), respectively.

The excitation light from different sources (described in section 3.1.3) is guided to the setup through a single or multimode fiber (1). The beam is then collimated by an aspheric lens and directed towards a 10:90 neutral density filter (2) such that 10% of the beam intensity is focused on the sample (mounted on a piezo x-y-z stage from Newport described in section 3.1.4 (5)) through an IR objective with a NA of 0.42 and a working distance of 20 mm (4). The 90% of light reflected by the density filter reaches a powermeter (described in section 3.1.5) in order to control the power on the sample. The PL collected from the sample, as well as a reflected fraction of the laser light goes back through the microscope objective and about 90% of the intensity is reflected by the neutral density filter (2) in the spectrometer (7) direction, where the sample reflected laser light is blocked by a long wavelength pass filter with a cutoff wavelength of 1150 nm (6). The sample is imaged using white light (11) directed towards the sample through a flip 45:55 pellicle beam splitter (3) and through the objective (4). The light reflected from the sample is reflected by a fixed pellicle beamsplitter (8) and focused (9) on a

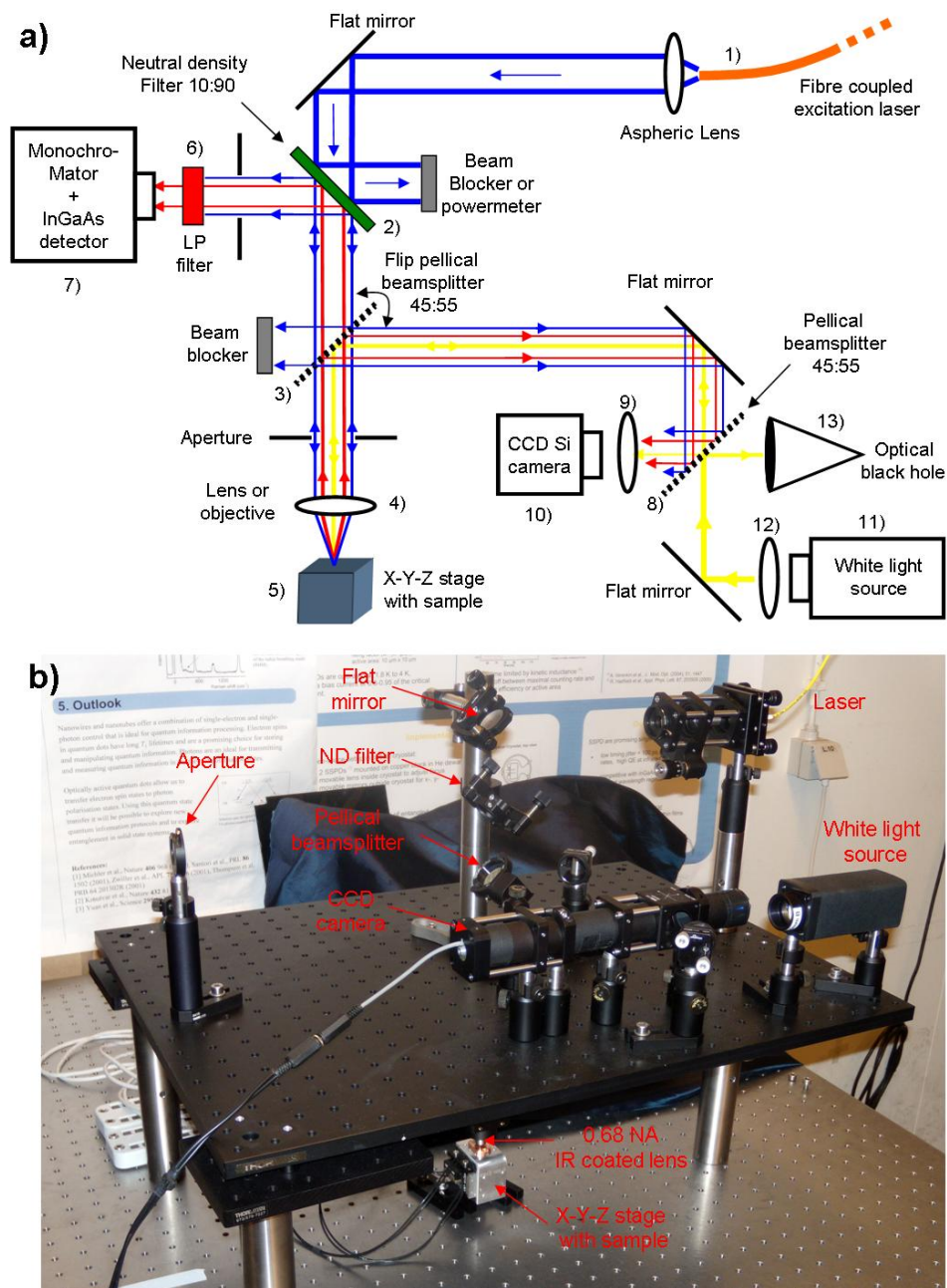


FIGURE 3.1: a) Schematics of the home built confocal microscope setup. b) Picture of the confocal microscope setup mounted on a dedicated optical table. The monochromator with a fitted InGaAs detector lies on the same table, optically aligned with the setup (on the left, not shown on this picture)

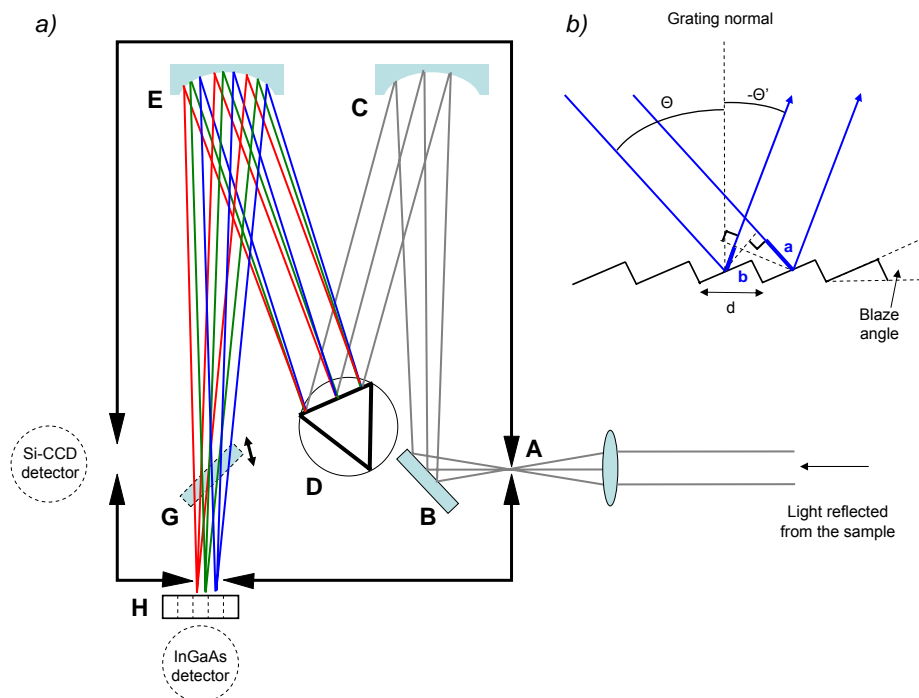


FIGURE 3.2: Schematic of the monochromator

CCD camera (10). The quality of the image is dramatically improved by the use of an optical "black hole" (13) to avoid that light coming directly from the white light source disturbs the image. The spectrometer is connected to a PC, via USB connection, in order to control the mirrors and gratings inside.

On Figure 3.1 b) the setup in its earlier state can be seen. The sample scanning is made possible through a moving stage that has three degrees of freedom, and which is controlled via the serial COM port of a PC. In general most of the control software was written in MATLAB.

3.1.2 Spectrometer

The detection part of our setup consists of a nitrogen cooled InGaAs detector array fitted to a monochromator. The Princeton Instruments Oma V detector [24] consists of a linear array of 512 InGaAs photodiodes able to detect light with a wavelength ranging from $0.8 \mu\text{m}$ to $1.7 \mu\text{m}$. The monochromator is a Spectra Pro 750 with an aperture ratio $f/9.7$ corresponding to a NA of about 0.05, or an acceptance angle of $2 \cdot 2.9^\circ$ ¹. A schematics of the spectrometer and the InGaAs detector can be seen in Fig. 3.2 a.).

¹ $\frac{f}{\#} = \frac{1}{2 \cdot NA}$, $NA = n \cdot \sin \theta$

The fundamental operation principle of the spectrograph is described in the following paragraph. A collimated light beam coming from the confocal microscope setup is focused at the entrance slits (A) by an $f = 5$ cm lens. The choice of the focal length of the lens is dictated by the f-number of the monochromator ($f/9.7$) and the diameter of the collimated light beam. The light rays that passed through the slit are directed through a planar mirror (B) onto a parabolic mirror (C), which reflects the incident rays in a collimated beam. This collimated beam is then diffracted by a grating (D), which disperses light with different wavelengths with different corresponding angles.

The dispersed light rays with different wavelengths are finally focused by a second parabolic mirror (E) on different spatial locations along the InGaAs array (H). Thus a spectrum of the light intensity as a function of the wavelength can be obtained. Note: in our setup two detectors were available: an InGaAs detector and a Si CCD detector. The selection of the detector was made through a flip-mirror (G).

A more detailed description of gratings physics is given in this paragraph. The cross-section of a ruled grating surface with incident and diffracted rays is shown in Fig. 3.2 b.). In principle a ruled grating consists of a substrate material (typically crystal silicon substrate or fiber-glass) with a large number of parallel grooves, coated with a reflecting material such as aluminium. On the figure two rays of the same wavelength travel parallel to each other and impact the grating on two neighboring grooves. A maximum of intensity occurs, when the two refracted rays have the same phase. Therefore, the location of intensity maxima can be calculated, from the path difference between the rays:

$$\begin{aligned}
 n \cdot \lambda &= a - b = \\
 &= d \cdot \sin(\theta) - d \cdot \sin(\theta') \\
 &= d(\sin(\theta) - \sin(-\theta')) = \\
 &= d(\sin(\theta) + \sin(\theta'))
 \end{aligned} \tag{3.1}$$

Where d is the groove spacing, λ the wavelength, θ and θ' the angles measured from the grating normal for the incident and reflected angles, respectively and n is an integer, which corresponds to different diffraction orders of a grating (we usually only work with the first order, $n = 1$).

Eq. 3.1 is known as the grating equation. Dispersion, which refers to the angle in which the same spectrum is spread can be deduced quantitatively from the grating equation and is found to be inversely proportional to d , the grating constant.

$$\frac{d\theta'}{d\lambda} = \frac{m}{d \cdot \cos \theta'} \quad (3.2)$$

Thus, for a grating with a high (low) groove density the dispersion will be large (small), and consequently the resolution will be high (low) but with lower (higher) intensity. The blaze angle (Fig. 3.2 b.)) determines the efficiency curve of a grating. For example, a grating "blazed" at $1,3 \mu\text{m}$ will have its maximum efficiency at this wavelength.

In our setup, 3 different gratings are mounted on a turret (D). These gratings have the following parameters: 1) 85 g/mm, "blazed" at $1,3 \mu\text{m}$, 2) 600 g/mm, "blazed" at $1,6 \mu\text{m}$ and 3) 1800 g/mm, "blazed" in the visible, with the software (WinSpec), a setting is available to change the grating in use and the center wavelength of the detected spectrum.

The InGaAs detector, consisting of an array of 512 photodiodes, is characterized by different parameters. An important one is called dark noise. There are two sources of dark noise: first, the reverse bias leakage current, which is due to minority carrier diffusion and secondly thermally activated carriers.

To decrease the dark noise, the array is cooled down via a cryostat filled with liquid nitrogen. Once the sensor's temperature drops to approximately $-100 \text{ }^{\circ}\text{C}$ the system is ready for measurement.

Statistically dark noise is random and since its distribution is even, it can be subtracted from the measured signal in order to increase signal to noise ratio. For this a background of the dark noise is recorded before measurement (slit closed) and the software automatically subtracts it from the signal.

An important measurement parameter is the integration time, which determines the amount of time elapsed to record a spectrum. Since dark noise is completely random an integration time twice as long increases the signal to noise ration by a factor of $\sqrt{2}$, thus long integration times (1 minute or more) are helpful, to get "cleaner" SWCNT PL spectra. Shorter integration time is used when scanning a sample, in order to shorten the measurement time.

3.1.3 Lasers

In the laboratory I had access to two laser sources: a Mira 900 and a Spectra Physics 3900. The Mira 900 is a mode locked ultrafast laser that uses Titanium:sapphire as the gain medium. It is tunable from 710 to 1000 nm. There are two modes of operation for this laser: the low power configuration uses 8 Watts and the high power 12 Watts from the pump laser (Verdi). The emitted laser power is 500 mW and 1100 mW, respectively. The output polarization is horizontal in every mode. The 3900 manufactured by Spectra Physics also uses Titanium-doped sapphire as the gain medium. The peak intensity is reached at 790 nm. An average output power of 2.5 W can be reached with a pump power of 20 W. The polarization is horizontal for all operation modes.

It can be shown that the 700 nm-1000 nm range of these lasers fits with the E_{22} , transitions of small diameter (< 1.2 nm) SWCNTs emitting in the available InGaAs detection range (900-1600 nm).

3.1.4 Motors

During my experiments I used two types of motors: 3 piezo-motors (from Newport) and a stepper motor (from Standa). The piezo-motors have been used to manipulate the sample stage with a 50 nanometer precision, although this was not a reproducible movement, since the motor operated in an open-loop. The stepper motor was used to change the wavelength of the laser. Both of the motors were automated from a Matlab routine via the serial interface of the computer. The implementation codes can be found in Appendix A.

3.1.5 Power meter

A power meter (Thorlabs PM100) was used in order to measure the laser power density on the samples. The readout range of the power meter depends on the sensor in use. In the laboratory we had access to sensors to read power ranging from 50 nW up to 20 W, with a 12 bit resolution. The read-out of the power meter as well as the tuning of measurement parameters (e.g λ range) could be computer-controlled via the serial port.

3.2 Description of the measurement procedures

The focus of my thesis is the optical investigation of carbon nanotubes. My tasks included:

- Find a nanotube manually, for the purpose of optimizing the detection parameters.
- Sample mapping, in order to get a map of the position of optically active SWCNTs on a large area (mm \times mm).
- PLE mapping, in order to assign chirality of a SWCNT

These three tasks are implemented in two Matlab GUIs (one for manual search and sample mapping, the second one for PLE mapping) that I want to describe below briefly.

3.3 PLE mapping automatization

As described earlier in the theory section, semiconducting nanotubes can be excited in their E_{22} transitions and emit light in the E_{11} transition. When the excitation photons have exactly the same energy as the E_{22} transition, we say that they are resonant. In this case the emission intensity is the highest. It would then be very useful to record the emission wavelength and intensity as a function of the excitation wavelength. Such a measurement output is called a photoluminescence excitation (PLE) map.

To realize this, I controlled the excitation wavelength of the Mira 900 or the Spectrum Physics 3900 lasers with a step motor (section 3.1.4) connected to the micrometer control of the laser with a belt. The step-motor is controlled via the USB port by a control box. The range and velocity wavelength change rate are controlled from a Matlab GUI that I wrote, using a DLL package to command the control box. I calibrated the motor so that the wavelength change is a linear function of the number of steps. Since the output power of the laser is not constant over the full NIR range, I had to normalize each recorded spectrum. For this I read the power on the sample (indirectly from the reflected power, see Fig. 3.1 a)) from the power meter via the RS-232 port. A flowchart of the GUI program is shown in Fig. 3.3.

Upon initializing, the user has to reset the current stepper motor position, which will be associated with the current wavelength. From this point on the program is able to calculate the current wavelength, based on the ratio that I measured (the slope of the step position vs. wavelength

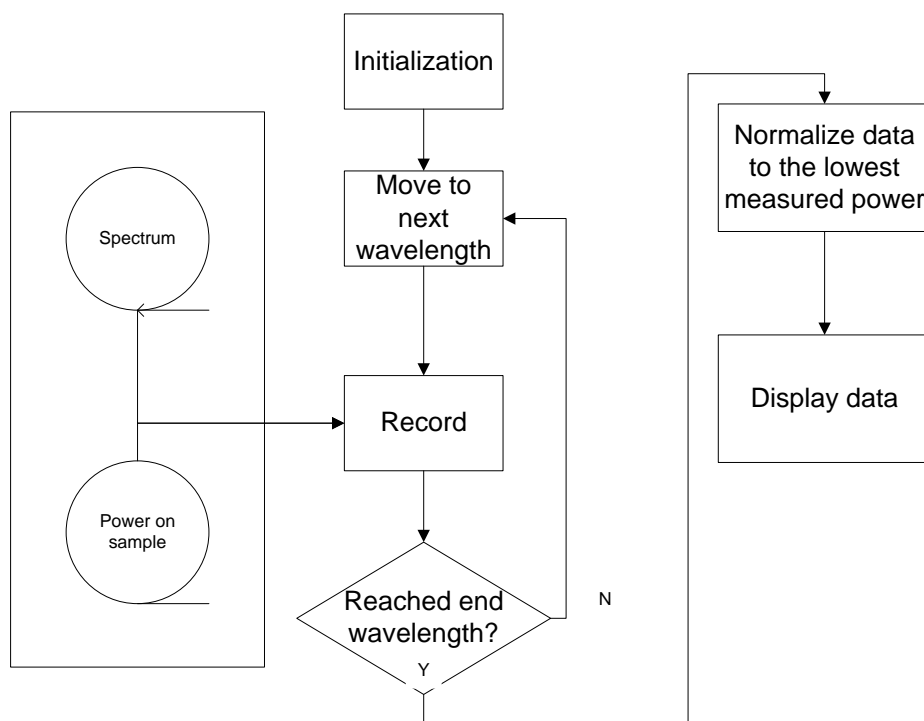


FIGURE 3.3: Flowchart of the PLE automatization

line). The program allows the user to move to a certain wavelength, or to a certain position. The PLE map generation needs only 3 parameters: the starting and the end wavelength and the step size, which determines the resolution of the PLE map.

To calculate the power density the area of the beam had to be calculated. For this I wrote a software that utilizes the CCD camera image through an image processing algorithm. The image taken by the CCD camera is first converted, so it can be manipulated in MATLAB. In Matlab the user has to select an X or Y coordinate, along which a cross-section will be made through the beam. From the cross-section the beam's diameter can be determined in the scale of pixels. To convert this to a micrometer scale I used a calibration sample, in order to find out the conversion ratio.

3.3.1 Manual search and sample mapping

As described earlier, the sample with suspended nanotubes is positioned on a x-y-z stage actuated by three piezo steppers from Newport (AG LS-25) with a specified minimum step size of 50 nm. These steppers are operated in open loop and the step size is therefore not reproducible.

The GUI that we developed in Matlab to control the piezo steppers via the serial communication port for manual search and sample mapping is shown in Appendix B. Each direction can be set with three different step sizes (low, medium, high). The motors are equipped with an odometric position feedback, therefore we are able to track the movement of the stage precisely (after compensating the motors). After locating a starting point for our scan we have to reset the positioning so we know how far we are on our sample. This has to be done, because it is not possible to record a spectrum and to image with the CCD camera at the same time.

For sample mapping, the user can input the amount of steps to be scanned in X and Y directions, with the amount of "piezo-steps" in each step. Since the backward and forward direction steps are intrinsically different, we have to compensate to minimize the drift in imaging. The scanning takes place first from the left to right than from the right to the left, in a meander shape. The sequence consists of 4 stages: first the motors move to the next location, then the program waits for the motors to reach their destination and for all the drift effects to die out. Next, the spectrum gets recorded, therefore the program has to maintain communication with the spectrograph's motherboard. This is done via an ActiveX Server initialized from Matlab. Depending on the integration time set in WinSpec (the GUI for the control of the spectrograph, provided by Princeton Instruments), the program waits for the execution and after waiting and additional time, the sequence repeats itself.

When the final destination is reached the program stops. All the spectra taken during the process are stored in a folder, in a format that is custom to Princeton Instruments, with the extension .SPE, which contains a header with information about the whole experiment (date, sensors used, grating and mirror positions, dark noise, etc.).

The final data set of a sample mapping consists of a 3-dimensional matrix with the position in x-y and the spectra in z. It is then possible to scroll through in z to obtain x-y maps at different emitted wavelengths.

Chapter 4

Results

4.1 Locating SWCNTs

My first task was to locate SWCNTs on different samples. For this, I used the equipment described in Chapter 3. Although the density of nanotubes on the sample is relatively large, only a very small proportion can be detected. This is due to the following reasons:

- In average, only 2/3 of nanotubes in a batch are semiconducting, i.e. having a band gap. The other 1/3 are metallic and can only emit light in very special conditions [25].
- Among the 2/3 of semiconducting nanotubes, only small diameter ones (< 1.2 nm approximately) emit in the detection range (900 nm - 1600 nm) of our InGaAs array. We do not have a statistical distribution of the tube diameter available, but based on the experience in growing tubes in the group, it is thought that the probability to get $d < 1.2$ nm is less than 10%.
- Furthermore, as a function of the trench width or pillar pitch, the probability to get entangled tubes or bundles is relatively high [22]. If small diameter semiconducting tubes are bundled with larger diameter tubes, it has been shown that the excitons generated in these tubes diffuse to larger diameter ones and recombine by emitting photons out of detection range. If metallic tubes are present in the bundle, they can quench the PL [26].

All these points together make the detection of a single SWCNT very challenging.

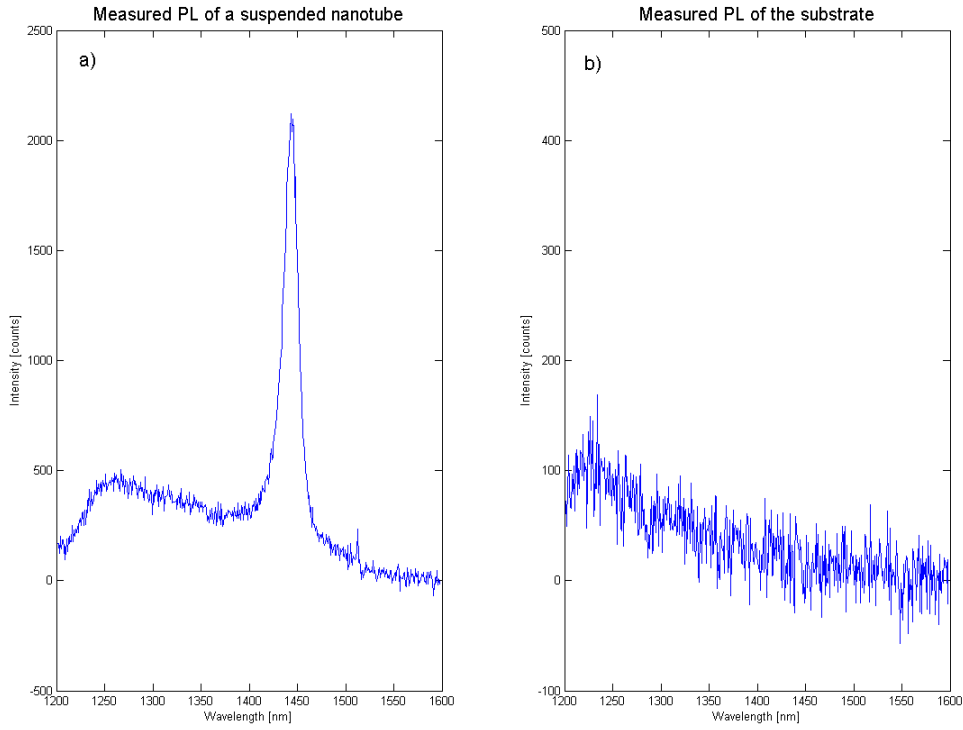


FIGURE 4.1: Measured photoluminescence. a.) SWCNT found b.) no tube in the spot area

The search for a SWCNT was done manually in a first step. Figure 4.1 shows two spectra: a) An optically active nanotube was lying under the beam, (integration time 60 seconds). Next to the PL signal of the nanotube around 1440 nm, the edge of a peak can be seen around 1250 nm, which is due to PL from the Si substrate luminescence. SWCNTs luminescing below 1250 nm are therefore more difficult to detect. On b), a spectrum, where no optically active tube is lying in the beam. Only the PL from the substrate is visible.

Figure 4.2 a) shows a PL spectrum from an individual SWCNT with a higher integration time in order to increase the signal to noise ratio (60 s integration time). The spectrum shows a peak at 1455 nm corresponding to 852 meV (conversion formula in footnote)¹. This peak shows the characteristic asymmetric line shape with a sharp rise on the low energy side (larger wavelength) and a more gradual fall off to zero at high energies (lower wavelength), consistent with the shape of van Hove singularities (VHS) in the joint density of states [27]. From a lorentzian fit, the full width at half maximum is found to be about 16 meV. The resonant nature of the photoluminescence intensity can be checked by varying the Ti:sapph laser wavelength while

$${}^1 E[eV] = h\nu = \frac{hc}{\lambda} = \frac{4.136 \cdot 10^{-15} \text{ eV} \cdot \text{s} \cdot 2.998 \cdot 10^8 \text{ m} \cdot \text{s}^{-1}}{\lambda(\text{m})} = \frac{1,23}{\lambda}$$

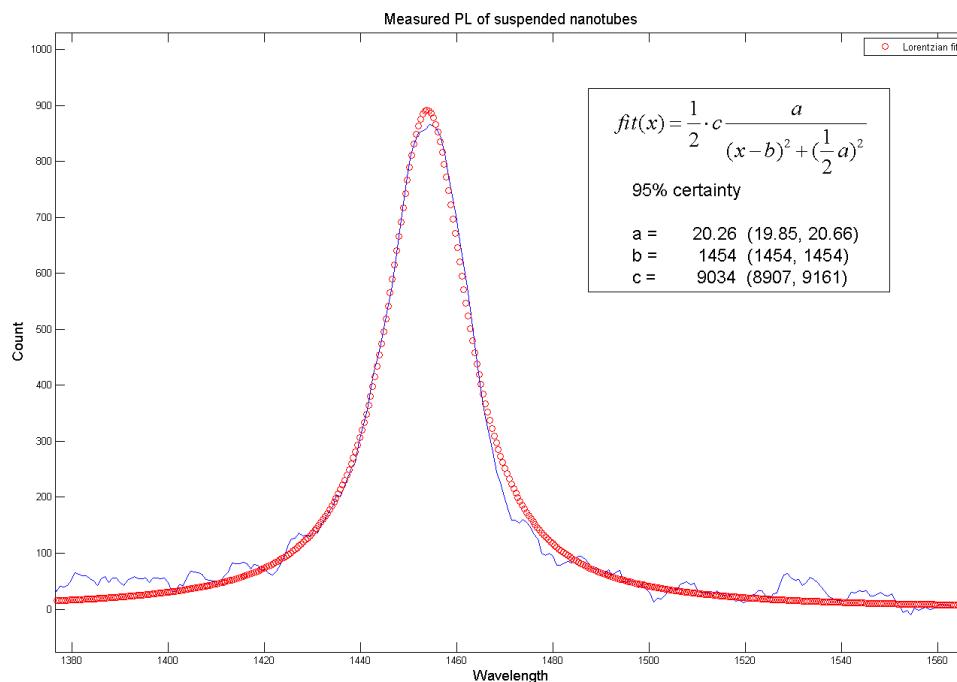


FIGURE 4.2: Photoluminescence spectrum of a nanotube with a Lorentzian-fit

recording the emission spectra. The result of these measurements is called a PLE map. PLE maps are very useful to assign the chirality of nanotubes and will be discussed later in this chapter.

Once a nanotube is found, the focus distance, i.e. the distance between the tube and the objective has to be optimized in order to get the maximum signal in the monochromator. This corresponds to a nearly collimated beam before the monochromator lens (see Fig. 3.1 a)). The focus was first set to get the sharpest white light image. From basic optical knowledge it is known that light with longer wavelength focuses further from the lens. For this reason I increased the distance between the stage and the objective until I reached the maximum intensity. In terms of piezo-steps, this distance has been found around 30 and 55 in low resolution.

I repeated the optimization process on more than 10 nanotubes distributed over the sample. Initially the beam size was too small, making the search for a tube even more difficult. One of the improvements that had to be made to the setup was the implementation of a lens positioned at twice the focal length from the objective aperture. This leads to a defocusing of the beam, giving rise to a larger spot size. Figure 4.3 shows the setup alteration that has been implemented in order to increase the probability of presence of a nanotube under the laser spot during scanning.

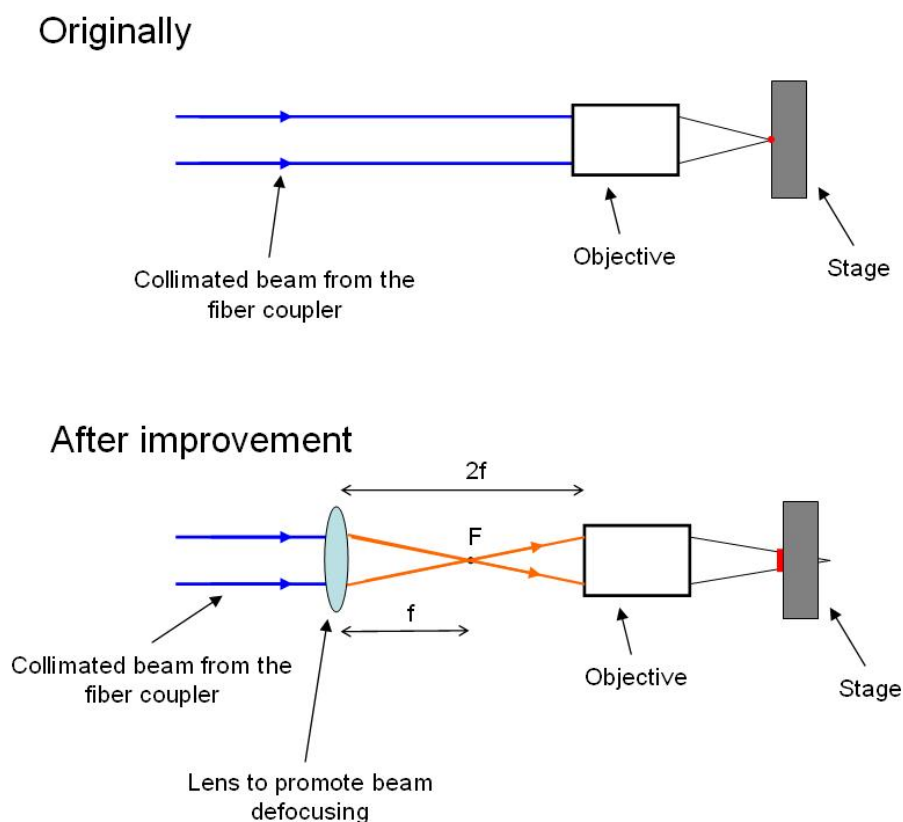


FIGURE 4.3: Setup modification in order to increase the beam size

An important parameter for PL measurements is the power density applied on the sample. To precisely tune the power density, the power on the sample and the size of the laser spot have to be measured.

The power can be measured precisely using the parameters described in Chapter 3. The problem arises, when the beam area has to be measured. The measurement of the laser spot diameter is made from a line cut in the CCD camera image processed in MATLAB, as show in Fig. 4.4. The laser power had to be decreased to minimum to ensure that the CCD camera did not saturate. The MATLAB algorithm that I wrote can be found in Appendix A (`getbeam.m`). In the case where the beam was defocused, we measured a beam diameter of $11.9 \mu\text{m}$, while the original beam size was measured to be only $8 \mu\text{m}$ for a wavelength of 820 nm with the laser coupled to a multimode fiber. Thus the optimal power on the sample in these conditions was calculated to be 0.63mW and 1.41mW , respectively.

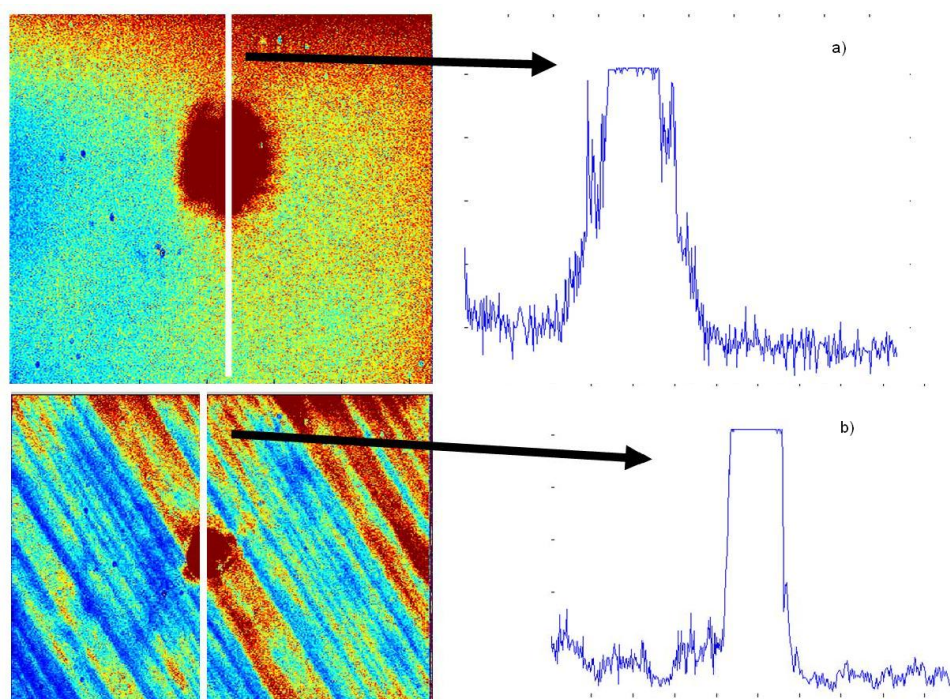


FIGURE 4.4: Beam diameter measurement from the CCD image a) beam with lens, b) beam without lens

4.2 The aging effect of SWCNTs

During the measurement process, I came across a noticeable effect: the decay of the PL intensity over time. This effect has been observed for all investigated nanotubes on different samples. Fig. 4.5 shows a graph of the intensity in counts/s as a function of the time for a SWCNT excited at 860 nm (close to resonance) under a power density of about 0.44 kW/cm^2 . The intensity decreased by a factor 10 after about 3h of excitation.

The plot in Fig. 4.6 shows the time elapsed under continuous excitation at 860 nm to reach an intensity decrease of a factor 10 as a function of the power density for four nanotubes. It suggests a quicker decay with higher power density. A similar behavior has been observed by another group at Queen University in Canada. They observed differences in PL decay as a function of the relative humidity. A low relative humidity of 15-20% reduced the incidence of aging [28].

Another reported source of PL decay is the collapse of the nanotubes under purely optical forces (with power densities of the order of MW/cm^2), either from photon momentum transfer,

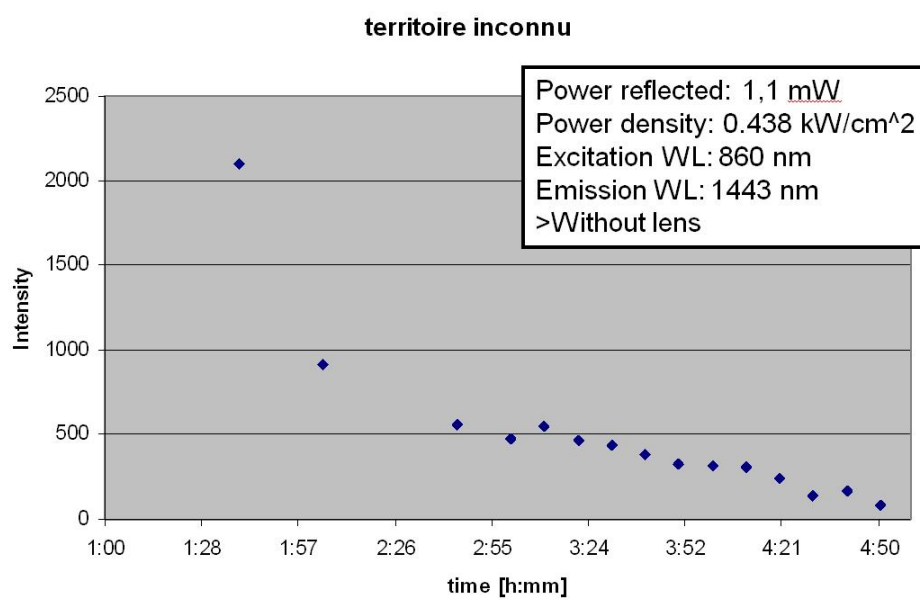


FIGURE 4.5: The degradation of the PL signal from an individual SWCNT over time

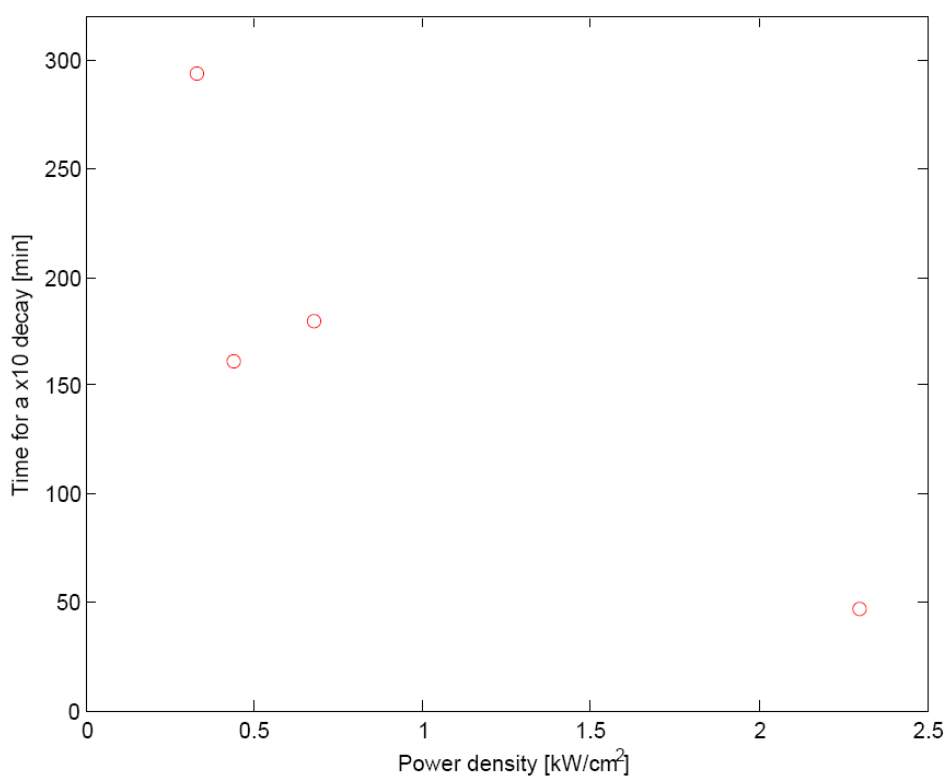


FIGURE 4.6: The time elapsed under continuous excitation at 860 nm to reach an intensity decrease of a factor 10 as a function of the power density for four nanotubes

or from the induced dipole gradient [29]. From the reported power densities, we think that in our case the effect of humidity is more likely to be the main source of decay.

This effect prevents long measurements like PLE maps (see next sections) and has to be minimized in future experiments. This can be done by working with the sample in a vacuum chamber purged and filled with a nitrogen atmosphere for example [28].

4.3 Sample mapping

Here the goal is to provide a map of the position of optically active nanotubes on a macroscopic area (typically a few mm^2) using the program described in section 3.2.3. A good trade off between the time needed to record such a map and the spatial resolution has to be found. In the map shown in Fig. 4.7, the scanning area is about $200 \mu m \times 200 \mu m$, with approximately 3500 points in each x and y directions. The integration time is set to 2 s (which is the inferior limit in order to clearly identify the PL of a tube out of the noise) and the excitation wavelength is set to 820 nm. The choice of the excitation wavelength determines the tube chirality we are looking for. 820 nm does not correspond to any resonant wavelength, but doing so we include several chiralities with a resonant excitation close to 820 nm, i.e. (13,2), (12,4) and (11,6).

Since the integration time is set at the limit of detection in the map shown in Fig. 4.7, it is difficult to attribute the spots to SWCNTs. Also, at this stage of development the setup could not be used yet to trace back the tubes since the piezo motors are working in open loop, i.e. the step size is not reproducible. Another difficulty is the fact that the sample is always tilted in a small amount, giving rise to change in focus, i.e. change in intensity at the monochromator slits, between the lowest and highest positions. This can be compensated by actively changing the focus during the scan.

4.4 PLE mapping

Once an optically active nanotube is found, the next step is to assign its chirality. For this I recorded a PLE map using the GUI described in Chap. 3. Fig. 4.8 c) shows a typical PLE map recorded on the NRC sample. The emission wavelength is recorded in the range 1200 nm - 1600 nm and the excitation is swept from 750 nm to 900 nm with 5 nm steps. The integration time is 2 seconds. Below 1270 nm, the emission from the Si substrate is clearly visible. The maximum

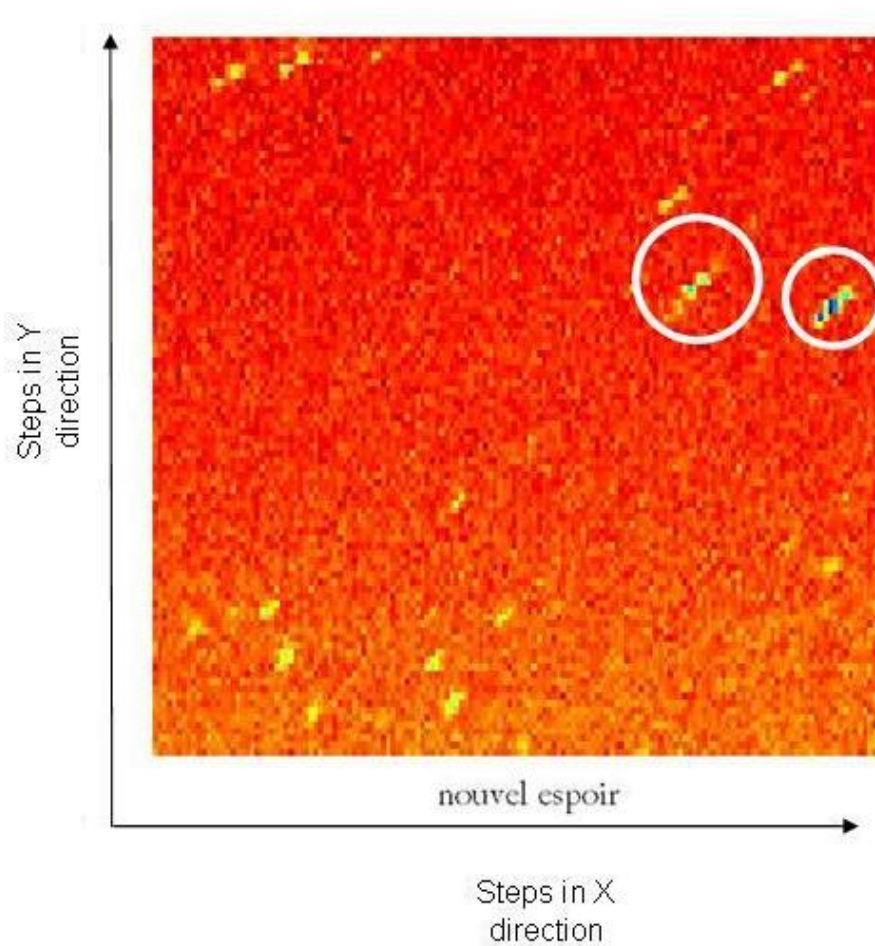


FIGURE 4.7: Mapped samples with possible nanotubes

intensity for the nanotube is recorded at an emission wavelength of about 1375 nm and for an excitation wavelength of about 855 nm.

From these two values, it is possible to assign the chirality of the nanotube. Indeed, Bachilo et al. studied SWCNTs suspended in micelles and could provide assignment tables from a comparison of their results with Raman spectroscopy on individual SWCNTs [30]. This table can be found in Appendix C. However, it is not possible yet to assign our nanotube. Indeed, it has been reported that the direct environment of individual nanotubes shifts the E_{22} and E_{11} transitions.

Lefebvre et al. found that emission peaks are blueshifted by 28 meV on average for the suspended nanotubes as compared to the encapsulated nanotubes. Similarly, the resonant absorption peaks at the second set of van Hove singularities are blueshifted on average by 16meV. Considering this small shifts, I found the best match for the tube in Fig. 4.8 to be (11,6). The spectrum

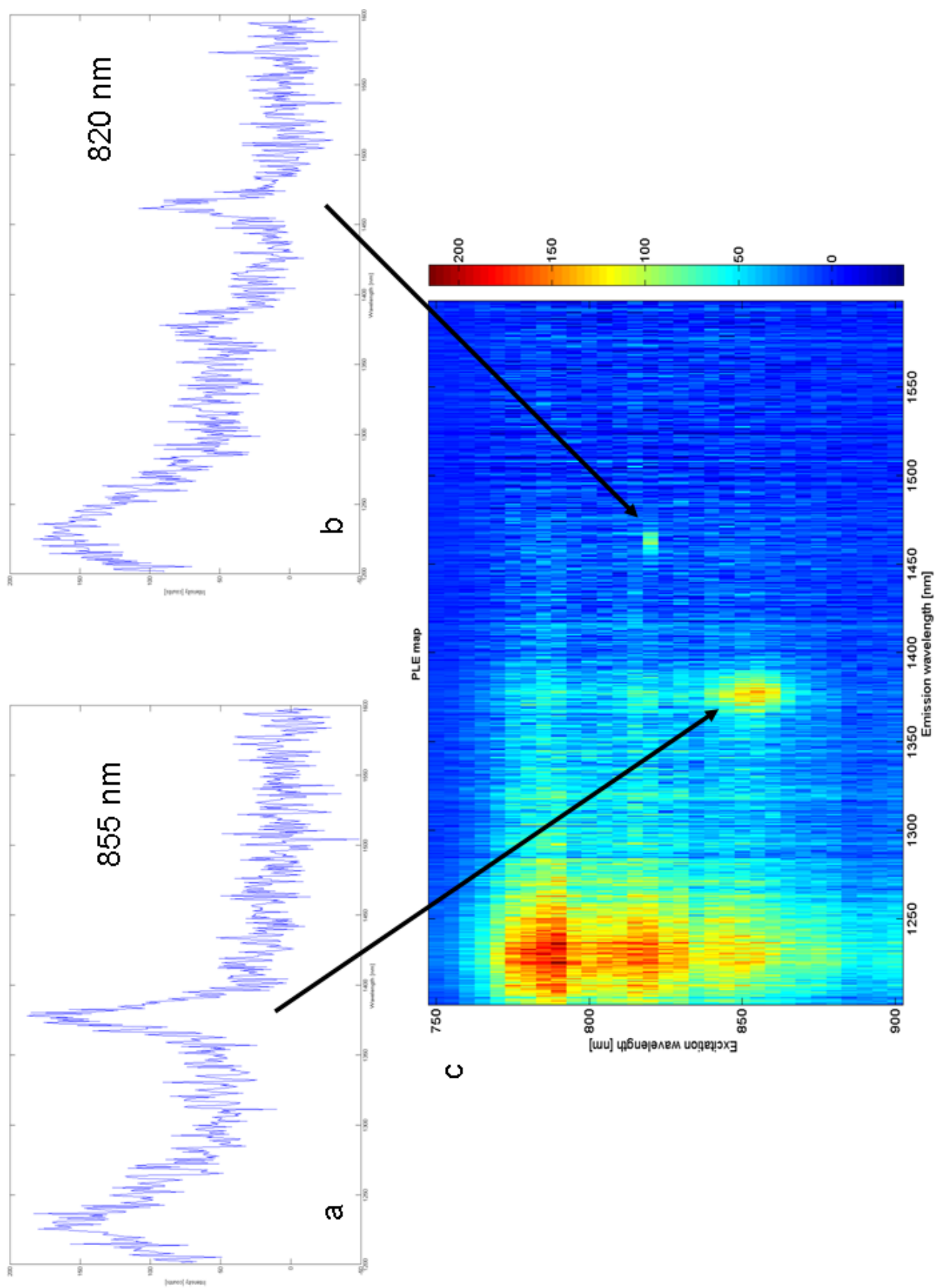


FIGURE 4.8: PLE map of a (11, 6) individual nanotube (c), with cross-sections at 855 nm (a) and 820 nm (b)

of this tube recorded at an excitation wavelength of 855 nm is displayed in panel a). A small spot is also visible at an emission wavelength of 1510 nm and excitation wavelength of 820 nm. The spectrum displayed in panel b) at an excitation wavelength of 820 nm shows a peak shape similar to the one of a nanotube. The best match would then be a (12,5).

It is important to note that we recorded a higher resolution PLE map of the (11,6) nanotube prior to the shown map and the supposed (12,5) tube was not present. It might be a tube that became optically active for a reason we don't really understand. With a longer integration time and smaller steps in excitation wavelength, we would get a better quality PLE map. However, such long measurements would be strongly limited by the aging effect for tubes in ambient conditions we described earlier in section 4.2.

Chapter 5

Conclusion and Outlook

5.1 Conclusion and outlook

In this work, I measured the photoluminescence of individual single wall carbon nanotubes from different samples with a home made experimental setup. The most important part of my work was to implement routines in Matlab in order to automatize the search of optically active nanotubes as well as PLE mapping to assign the chirality of the tubes I found. I also modified the "hardware" part of the setup to enlarge the laser spot size on the sample in order to facilitate the tube searching process.

I observed an aging phenomenon characterized by a decay of the PL from individual tubes. The decay rate increased with the power density excitation. From the available literature, I attributed this effect to the relative humidity in the direct environment of the suspended nanotubes.

In the future, several improvements have to be made in order to allow more in-depth investigations of the optical properties of suspended nanotubes. This will be useful to design and study future nanotube-based optoelectronic devices, especially ultraclean nanotube devices developed in the Quantum Transport group using a new technology [31].

Some of the possible improvements are:

- Using closed loop piezo motors in order to have a reproducible positioning system. A beam scanner using galvo mirrors is to be considered as well. This would allow quicker record of spatial maps as well as a higher flexibility in the beam scanning.

- Include a system that allows a cleaner and dryer environment of the tubes, in order to minimize or even suppress the aging effect. This can be realized by the implementation of a vacuum chamber with gas inlets for flushing. This vacuum chamber could be easily converted to a cryostat allowing low temperature measurements.
- In this work, we did not perform polarization measurements. For this we need to setup polarizers and wave plates.

Appendix A

Program codes

A.1 RT_Setup.m

```
1 % -----
2 % -----
3 %           Automization RT_setup @ Vlab
4 %
5 %           Gilles Buchs and David Lakatos
6 %           November 2009, TU Delft
7 % -----
8 % -----
9
10
11 function varargout = RT_setup(varargin)
12
13 % Begin initialization code - DO NOT EDIT
14 gui_Singleton = 1;
15 gui_State = struct('gui_Name',       mfilename, ...
16                   'gui_Singleton',  gui_Singleton, ...
17                   'gui_OpeningFcn', @RT_setup_OpeningFcn, ...
18                   'gui_OutputFcn',  @RT_setup_OutputFcn, ...
19                   'gui_LayoutFcn',  [], ...
20                   'gui_Callback',   []);
21 if nargin && ischar(varargin{1})
22     gui_State.gui_Callback = str2func(varargin{1});
23 end
24
25 if nargout
26     [varargout{1:nargout}] = gui_mainfcn(gui_State, varargin{:});
27 else
```

```
28     gui_mainfcn(gui_State, varargin{:});
29 end
30 % End initialization code - DO NOT EDIT
31
32
33 % -----
34 %             RT_setup_OpeningFcn
35 % -----
36 %
37 % --- Executes just before RT_setup is made visible.
38 function RT_setup_OpeningFcn(hObject, eventdata, handles, varargin)
39
40 clc;
41 % Choose default command line output for RT_setup
42 handles.output = hObject;
43
44 % Default jog speed (3 = high speed)
45 handles.speed=3;
46
47 % Default Z speed (3 = high speed)
48 handles.speed_Z=3;
49
50 % Initialization Button Stop
51 handles.stop=0;
52
53 % Define action when one wants to close the GUI
54 set(handles.figure1, 'CloseRequestFcn', @closeGUI);
55
56 % Define action when different radiobuttons in XY are selected
57 set(handles.Speed_Panel_buttongroup, 'SelectionChangeFcn', ...
58     @Speed_Panel_buttongroup_SelectionChangeFcn);
59
60 % Define action when different radiobuttons in Z are selected
61 set(handles.Speed_Z_Panel_buttongroup, 'SelectionChangeFcn', ...
62     @Speed_Z_Panel_buttongroup_SelectionChangeFcn);
63
64 % Define action when different togglebuttons in MODES are selected
65 set(handles.MODE_buttongroup, 'SelectionChangeFcn', ...
66     @MODE_buttongroup_SelectionChangeFcn);
67
68 % Define action when different radiobuttons in Detector are selected
69 set(handles.Detector_buttongroup, 'SelectionChangeFcn', ...
70     @Detector_buttongroup_SelectionChangeFcn);
71
72 % Initialization number of clicks on serial port gestion buttons
73 handles.Nb_click_open_XY=0;
74 handles.Nb_click_open_Z=0;
75 handles.Nb_click_close_XY=0;
```

```
76 handles.Nb_click_close_Z=0;
77
78 % Default wavelenght (index) value for map display
79 handles.sliderValue=1;
80
81 % Default value for detector pixels (InGas:512, Si:1340)
82 handles.pix=512;
83 handles.Max_slider=511;
84 handles.SliderStep=[0.00195 0.1];
85
86 % Update handles structure
87 guidata(hObject, handles);
88
89 % Close all open instruments
90 delete(instrfindall)
91 clear all
92 %
93 % -----
94
95
96
97 % UIWAIT makes RT_setup wait for user response (see UIRESUME)
98 % uiwait(handles.figure1);
99
100
101
102 % -----
103 %           RT_setup_OutputFcn
104 % -----
105 %
106 % --- Outputs from this function are returned to the command line.
107 function varargout = RT_setup_OutputFcn(hObject, eventdata, handles)
108 % Get default command line output from handles structure
109 varargout{1} = handles.output;
110 %
111 % -----
112
113
114
115
116
117 % -----
118 %           Control serial ports (piezos & InGaAs)
119 % -----
120 %
121 %
122 %
123 % --- Executes on button press in OpenXY.
```

```
124 function OpenXY_Callback(hObject, eventdata, handles)
125
126 handles.Nb_click_open_XY=handles.Nb_click_open_XY+1;
127 handles.Nb_click_close_XY=0;
128
129 if (handles.Nb_click_open_XY < 2)
130     set(handles.XY_status, 'String', 'OPEN');
131     set(handles.XY_status, 'BackgroundColor', [0.2,0.8,0]);
132     set(handles.XY_status, 'ForegroundColor', [1,1,1])
133     guidata(hObject, handles);
134
135 % Opens a serial communication object
136 global S1
137 S1=serial('COM5',...
138         'BaudRate', 921600, ...
139         'Parity', 'none', ...
140         'DataBits',8, ...
141         'StopBits', 1, ...
142         'FlowControl','none',...
143         'Terminator', 'CR/LF');
144     fopen(S1)
145 else
146     errordlg('Serial port already open','Error');
147 end
148 %
149 %
150 % --- Executes on button press in CloseXY.
151 function CloseXY_Callback(hObject, eventdata, handles)
152
153 handles.Nb_click_close_XY=handles.Nb_click_close_XY+1;
154 handles.Nb_click_open_XY=0;
155
156 if (handles.Nb_click_close_XY < 2)
157     set(handles.XY_status, 'String', 'CLOSED');
158     set(handles.XY_status, 'FontWeight', 'bold');
159     set(handles.XY_status, 'BackgroundColor', [1,0,0]);
160     set(handles.XY_status, 'ForegroundColor', [1,1,1])
161     guidata(hObject, handles);
162 %
163 global S1
164 fclose(S1);
165 delete(S1);
166 clear S1
167
168 else
169     errordlg('Serial port already closed','Error');
170 end
171 %
```

```
172 %
173 % --- Executes on button press in OpenZ.
174 function OpenZ_Callback(hObject, eventdata, handles)
175
176 handles.Nb_click_open_Z=handles.Nb_click_open_Z+1;
177 handles.Nb_click_close_Z=0;
178
179 if (handles.Nb_click_open_Z < 2)
180     set(handles.Z_status,'String','OPEN');
181     set(handles.Z_status,'FontWeight','bold');
182     set(handles.Z_status,'BackgroundColor',[0.2,0.8,0]);
183     set(handles.Z_status,'ForegroundColor',[1,1,1]);
184     guidata(hObject,handles);
185
186 % --- Opens a serial communication object
187     global S2
188     S2=serial('COM6',...
189             'BaudRate', 921600, ...
190             'Parity', 'none', ...
191             'DataBits',8, ...
192             'StopBits', 1, ...
193             'FlowControl','none',...
194             'Terminator', 'CR/LF');
195
196     fopen(S2);
197
198 else
199     errordlg('Serial port already open','Error');
200 end
201 %
202 %
203 % --- Executes on button press in CloseZ.
204 function CloseZ_Callback(hObject, eventdata, handles)
205
206 handles.Nb_click_close_Z=handles.Nb_click_close_Z+1;
207 handles.Nb_click_open_Z=0;
208
209 if (handles.Nb_click_close_Z < 2)
210     set(handles.Z_status,'String','CLOSED');
211     set(handles.Z_status,'FontWeight','bold');
212     set(handles.Z_status,'BackgroundColor',[1,0,0]);
213     set(handles.Z_status,'ForegroundColor',[1,1,1]);
214     guidata(hObject,handles);
215
216     global S2
217     fclose(S2);
218     delete(S2);
219     clear S2
```

```

220 else
221     errordlg('Serial port already closed','Error');
222 end
223
224
225 function Detector_buttongroup_SelectionChangeFcn(hObject,eventdata)
226
227 %retrieve GUI data, i.e. the handles structure
228 handles = guidata(hObject);
229
230 switch get(eventdata.NewValue,'Tag') % Get Tag of selected object
231     case 'InGaAs_radiobutton'
232         handles.pix=512;
233         handles.Max_slider=511;
234         handles.SliderStep=[0.00195 0.1];
235         display(handles.Max_slider)
236
237     case 'Si_radiobutton'
238         handles.pix=1340;
239         handles.Max_slider=1339;
240         handles.SliderStep=[0.001 0.1];
241         display(handles.Max_slider)
242
243     otherwise
244         % Code for when there is no match.
245         display 'Choose a speed'
246
247 end
248 %updates the handles structure
249 guidata(hObject, handles);
250
251 %
252 %
253 % -----
254
255
256
257
258 % -----
259 %             MODE: Remote or Local
260 % -----
261
262 function MODE_buttongroup_SelectionChangeFcn(hObject,eventdata)
263
264 global S1
265 global S2
266
267 switch get(eventdata.NewValue,'Tag') % Get Tag of selected object

```



```

268     case 'Remote_Mode_button'
269         fprintf(S1,'MR')
270         fprintf(S2,'MR')
271
272     case 'Local_Mode_button'
273         fprintf(S1,'ML')
274         fprintf(S2,'ML')
275
276     otherwise
277         % Code for when there is no match.
278         display 'Error'
279
280 end
281
282 % -----
283
284
285
286
287
288 % -----
289 %     Jog motion: manual acquisition of sample parameters (x_max_edit, y_max_edit)
290 % -----
291 %
292 %
293 % --- Executes on button press in X_right.
294 function X_right_ButtonDownFcn(hObject, eventdata, handles)
295
296 if (handles.Nb_click_open_XY  $\neq$  0)
297     global S1
298     fprintf(S1,'MR')
299     fprintf(S1,['1JA',num2str(handles.speed)])
300     set(handles.X_right,'String','X +')
301     set(handles.X_right,'BackgroundColor',[.2,0.8,0])
302
303     set(gcf,'WindowButtonUpFcn',{@ButtonUpFcn_X_right,handles});
304     guidata(hObject, handles);
305 else
306     errordlg('Serial port need to be open','Error');
307 end
308
309 function ButtonUpFcn_X_right(src,eventdata,handles)
310
311 global S1
312 fprintf(S1,'1ST');
313
314 %read step number in X
315 fprintf(S1,'1TP');

```

```
316 temp_steps=fscanf(S1);
317 temp_length=length(temp_steps);
318 handles.Nb_steps_X=char(1:temp_length);
319 for i=1:(temp_length-3)
320     handles.Nb_steps_X(i)=temp_steps(i+3);
321 end
322 set(handles.Pos_X_steps,'String',handles.Nb_steps_X)
323 set(handles.X_right,'String','X +')
324 set(handles.X_right,'BackgroundColor',[.925,0.914,0.847])
325
326
327 % --- Executes on button press in X_left.
328 function X_left_ButtonDownFcn(hObject, eventdata, handles)
329
330 if (handles.Nb_click_open_XY  $\neq$  0)
331     global S1
332     fprintf(S1,'MR')
333     fprintf(S1,['1JA-',num2str(handles.speed)])
334     set(handles.X_left,'String','X -')
335     set(handles.X_left,'BackgroundColor',[.2,0.8,0])
336
337     set(gcf,'WindowButtonUpFcn',{@ButtonUpFcn_X_left,handles});
338     guidata(hObject, handles);
339 else
340     error('Serial port need to be open','Error');
341 end
342
343 function ButtonUpFcn_X_left(src,eventdata,handles)
344 global S1
345 fprintf(S1,'1ST')
346
347 %read step number in X
348 fprintf(S1,'1TP');
349 temp_steps=fscanf(S1);
350 temp_length=length(temp_steps);
351 handles.Nb_steps_X=char(1:temp_length);
352 for i=1:(temp_length-3)
353     handles.Nb_steps_X(i)=temp_steps(i+3);
354 end
355
356 set(handles.Pos_X_steps,'String',num2str(handles.Nb_steps_X))
357 set(handles.X_left,'String','X -')
358 set(handles.X_left,'BackgroundColor',[.925,0.914,0.847])
359
360
361 % --- Executes on button press in Y_up.
362 function Y_up_ButtonDownFcn(hObject, eventdata, handles)
363
```

```

364 if (handles.Nb_click_open_XY  $\neq$  0)
365     global S1
366     fprintf(S1,'MR')
367     fprintf(S1,['2JA-',num2str(handles.speed)])
368     set(handles.Y_up,'String','Y +')
369     set(handles.Y_up,'BackgroundColor',[.2,0.8,0])
370
371     set(gcf,'WindowButtonUpFcn',{@ButtonUpFcn_Y_up,handles});
372     guidata(hObject, handles);
373 else
374     errordlg('Serial port need to be open','Error');
375 end
376
377 function ButtonUpFcn_Y_up(src,eventdata,handles)
378 global S1
379 fprintf(S1,'2ST')
380
381 %read step number in Y
382 fprintf(S1,'2TP');
383 temp_steps=fscanf(S1);
384 temp_length=length(temp_steps);
385 handles.Nb_steps_Y=char(1:temp_length);
386 for i=1:(temp_length-3)
387     handles.Nb_steps_Y(i)=temp_steps(i+3);
388 end
389
390 set(handles.Pos_Y_steps,'String',num2str(handles.Nb_steps_Y))
391 set(handles.Y_up,'String','Y +')
392 set(handles.Y_up,'BackgroundColor',[.925,0.914,0.847])
393
394
395 % --- Executes on button press in Y_down.
396 function Y_down_ButtonDownFcn(hObject, eventdata, handles)
397
398 if (handles.Nb_click_open_XY  $\neq$  0)
399     global S1
400     fprintf(S1,'MR')
401     fprintf(S1,['2JA',num2str(handles.speed)])
402     set(handles.Y_down,'String','Y -')
403     set(handles.Y_down,'BackgroundColor',[.2,0.8,0])
404
405     set(gcf,'WindowButtonUpFcn',{@ButtonUpFcn_Y_down,handles});
406     guidata(hObject, handles);
407 else
408     errordlg('Serial port need to be open','Error');
409 end
410
411 function ButtonUpFcn_Y_down(src,eventdata,handles)

```

```

412 global S1
413 fprintf(S1,'2ST')
414
415 %read step number in Y
416 fprintf(S1,'2TP');
417 temp_steps=fscanf(S1);
418 temp_length=length(temp_steps);
419 handles.Nb_steps_Y=char(1:temp_length);
420 for i=1:(temp_length-3)
421     handles.Nb_steps_Y(i)=temp_steps(i+3);
422 end
423
424 set(handles.Pos_Y_steps,'String',num2str(handles.Nb_steps_Y))
425 set(handles.Y_down,'String','Y -')
426 set(handles.Y_down,'BackgroundColor',[.925,0.914,0.847])
427
428
429
430 function Speed_Panel_buttongroup_SelectionChangeFcn(hObject,eventdata)
431
432 %retrieve GUI data, i.e. the handles structure
433 handles = guidata(hObject);
434
435 switch get(eventdata.NewValue,'Tag') % Get Tag of selected object
436     case 'High_radiobutton'
437         handles.speed=3;
438
439     case 'Medium_radiobutton'
440         handles.speed=2;
441
442     case 'Low_radiobutton'
443         handles.speed=1;
444
445     otherwise
446         % Code for when there is no match.
447         display 'Choose a speed'
448
449 end
450 %updates the handles structure
451 guidata(hObject, handles);
452
453
454
455 % --- Executes on button press in Reset_X_Button.
456 function Reset_X_Button_Callback(hObject, eventdata, handles)
457
458 if (handles.Nb_click_open_XY  $\neq$  0)
459     global S1

```

```

460     fprintf(S1,'1ZP');
461     set(handles.Pos_X_steps,'String','0');
462     set(handles.Pos_X_um,'String','0');
463     guidata(hObject, handles);
464 else
465     errordlg('Serial port need to be open','Error');
466 end
467
468 % --- Executes on button press in Reset_Y_Button.
469 function Reset_Y_Button_Callback(hObject, eventdata, handles)
470
471 if (handles.Nb_click_open_XY  $\neq$  0)
472     global S1
473     fprintf(S1,'2ZP');
474     set(handles.Pos_Y_steps,'String','0');
475     set(handles.Pos_Y_um,'String','0');
476     guidata(hObject, handles);
477 else
478     errordlg('Serial port need to be open','Error');
479 end
480
481
482
483
484
485 % -----
486 %     Focus Z motion
487 % -----
488 %
489 %
490 % --- Executes on button press in Z_up.
491 function Z_up_ButtonDownFcn(hObject, eventdata, handles)
492
493 if (handles.Nb_click_open_Z  $\neq$  0)
494     global S2
495     fprintf(S2,'MR')
496     fprintf(S2,['2JA',num2str(handles.speed_Z)])
497     set(handles.Z_up,'String','Z +')
498     set(handles.Z_up,'BackgroundColor',[.2,0.8,0])
499
500     set(gcf,'WindowButtonUpFcn',{@ButtonUpFcn_Z_up,handles});
501     guidata(hObject, handles);
502 else
503     errordlg('Serial port need to be open','Error');
504 end
505
506 function ButtonUpFcn_Z_up(src, eventdata, handles)
507 global S2

```

```
508 fprintf(S2,'2ST')
509
510 %read step number in Z
511 fprintf(S2,'2TP');
512 temp_steps=fscanf(S2);
513 temp_length=length(temp_steps);
514 handles.Nb_steps_Z=char(1:temp_length);
515 for i=1:(temp_length-3)
516     handles.Nb_steps_Z(i)=temp_steps(i+3);
517 end
518
519 set(handles.Pos_Z_steps,'String',num2str(handles.Nb_steps_Z))
520 set(handles.Z_up,'String','Z +')
521 set(handles.Z_up,'BackgroundColor',[.925,0.914,0.847])
522
523
524
525 % --- Executes on button press in Z_down.
526 function Z_down_ButtonDownFcn(hObject, eventdata, handles)
527
528 if (handles.Nb_click_open_Z  $\neq$  0)
529     global S2
530     fprintf(S2,'MR')
531     fprintf(S2,'2SU-43');
532     fprintf(S2,['2JA-',num2str(handles.speed_Z)])
533     set(handles.Z_down,'String','Z -')
534     set(handles.Z_down,'BackgroundColor',[.2,0.8,0])
535
536     set(gcf,'WindowButtonUpFcn',{@ButtonUpFcn_Z_down,handles});
537     guidata(hObject, handles);
538 else
539     errordlg('Serial port need to be open','Error');
540 end
541
542 function ButtonUpFcn_Z_down(src,eventdata,handles)
543 global S2
544 fprintf(S2,'2ST')
545
546 %read step number in Z
547 fprintf(S2,'2TP');
548 temp_steps=fscanf(S2);
549 temp_length=length(temp_steps);
550 handles.Nb_steps_Z=char(1:temp_length);
551 for i=1:(temp_length-3)
552     handles.Nb_steps_Z(i)=temp_steps(i+3);
553 end
554
555 set(handles.Pos_Z_steps,'String',num2str(handles.Nb_steps_Z))
```

```
556 set(handles.Z_down, 'String', 'Z -')
557 set(handles.Z_down, 'BackgroundColor', [.925, 0.914, 0.847])
558
559
560 % --- Select speed for Z motion.
561 function Speed_Z_Panel_buttongroup_SelectionChangeFcn(hObject, eventdata)
562
563 %retrieve GUI data, i.e. the handles structure
564 handles = guidata(hObject);
565
566 switch get(eventdata.NewValue, 'Tag') % Get Tag of selected object
567     case 'Low_Z_radiobutton'
568         handles.speed_Z=1;
569
570     case 'Medium_Z_radiobutton'
571         handles.speed_Z=2;
572
573     case 'High_Z_radiobutton'
574         handles.speed_Z=3;
575
576     otherwise
577         % Code for when there is no match.
578         display 'Choose a speed'
579
580 end
581 %updates the handles structure
582 guidata(hObject, handles);
583
584
585 % --- Executes on button press in Reset_Z_Button.
586 function Reset_Z_Button_Callback(hObject, eventdata, handles)
587
588 if (handles.Nb_click_open_Z  $\neq$  0)
589     global S2
590     fprintf(S2, '2ZP');
591     set(handles.Pos_Z_steps, 'String', '0');
592     guidata(hObject, handles);
593 else
594     errordlg('Serial port need to be open', 'Error');
595 end
596
597 % -----
598
599
600
601
602
603
```

```
604
605 % -----
606 %           Sample mapping
607 % -----
608 %
609 %
610 % --- Executes on button press in Stop_button.
611 function Stop_button_ButtonDownFcn(hObject, eventdata, handles)
612
613 if (handles.Nb_click_open_XY  $\neq$  0)
614     global S1
615     handles.stop=1;
616     fprintf(S1,'RS');
617     set(handles.Stop_button,'String','Stop')
618     set(handles.Stop_button,'BackgroundColor',[1,0,0])
619     set(handles.Run_button,'BackgroundColor',[0.925,0.914,0.847])
620
621     set(gcf,'WindowButtonUpFcn',{@ButtonUpFcn_Stop,handles});
622     guidata(hObject, handles);
623
624 end
625 function ButtonUpFcn_Stop(src,eventdata,handles)
626
627 set(handles.Stop_button,'String','Stop')
628 set(handles.Stop_button,'BackgroundColor',[.925,0.914,0.847])
629
630
631
632 % --- Executes on button press in Run_button.
633 function Run_button_ButtonDownFcn(hObject, eventdata, handles)
634
635 if (handles.Nb_click_open_XY  $\neq$  0)
636     global S1
637     set(handles.Run_button,'String','Run')
638     set(handles.Run_button,'BackgroundColor',[0.2,0.8,0])
639
640     % Creation of COM objects for communication with WinSpec
641     objExp = actxserver ( 'WinX32.ExpSetup' );
642     objDoc = actxserver ( 'WinX32.DocFile' );
643
644
645     % Acquisition sample area
646     X_max=str2num(get(handles.X_max_edit,'String'));
647     Y_max=str2num(get(handles.Y_max_edit,'String'));
648
649     % Acquisition mapping step size
650     Inc_X=get(handles.Step_Size_X_edit,'String')
651     Inc_Y=get(handles.Step_Size_Y_edit,'String')
```



```

652
653     curDate = fix(clock);
654
655     fid = fopen(strcat(get(handles.Edit_Path,'String'),'\_parameters.txt'), 'a');
656     fprintf(fid, '%d-%d-%d %d:%d\r\n\r\nXmax> %d, Ymax>%d\r\n\r\nXstep> %s, Ystep> %s\r\n\r\n', ...
657         curDate(1), curDate(2), curDate(3), curDate(4), curDate(5),...
658         X_max, Y_max, Inc_X, Inc_Y);
659     fclose(fid);
660
661     X_pos=0;
662     Y_pos=0;
663     Y_index=0;
664     stepCounter=0;
665
666     handles.stop=0;
667
668     set(handles.Pos_Map_X,'String',0);
669     set(handles.Pos_Map_Y,'String',0);
670
671     % Step size compensation
672     Step_back=get(handles.Step_back,'String');
673     fprintf(S1,['!SU-',Step_back]);
674
675
676     maxDelay = 1000; % this corresponds to 10sec delay
677     statusBit = 1;
678
679     while (Y_pos ≤ Y_max)
680         if mod(Y_index,2)==0
681             while (X_pos < X_max)
682                 % incremant the step counter
683                 stepCounter=stepCounter+1;
684
685                 % record a spectrum at pos: (X_pos,Y_pos) now with extra
686                 % debugging
687
688                 if objExp.Start ( objDoc )
689                     l = 0;
690
691                     fprintf(1,'\nOpened file! Right now @ step %d \n', stepCounter);
692
693                     while l < maxDelay
694                         statusBit = objExp.GetParam ( 'EXP_RUNNING' );
695                         if statusBit == 0
696                             fprintf(1, ...
697                                 '\nReady with creating spectrum, moving to next step');
698                             break;
699                         end

```

```

700         pause(0.01);
701         fprintf(1,'x');
702         l=l+1;
703     end
704
705     fprintf(1,'\n%d',l);
706     if l == maxDelay
707         fprintf(1, ['\n -----\n', ...
708             'Maximum delay exceeded! In file %d'], ...
709             stepCounter);
710         objExp.Stop();
711         pause(0.1);
712     end
713
714     objDoc.Close;
715 end
716
717 % Move in +X direction by Inc_X
718 fprintf(S1,['1PR',Inc_X])
719 wait_ready1(S1)
720 X_pos=X_pos+str2num(Inc_X);
721 set(handles.Pos_Map_X,'String',num2str(X_pos))
722
723 end
724 Y_index=Y_index+1;
725 else
726     while (X_pos>0)
727         % incremant the step counter
728         stepCounter=stepCounter+1;
729
730         % record a spectrum at pos: (X_pos,Y_pos) now with extra
731         % debugging
732
733         if objExp.Start ( objDoc )
734             l = 0;
735             while l < maxDelay
736                 statusBit = objExp.GetParam ( 'EXP_RUNNING' );
737                 if statusBit == 0
738                     break;
739                 end
740                 pause(0.01);
741                 l=l+1;
742             end
743             if l == maxDelay
744                 sprintf('Maximum delay exceeded! In file %d',num2str(stepCounter));
745             end
746
747             objDoc.Close;

```

```
748         end
749
750         % Move in -X direction by -Inc_X
751         fprintf(S1,['1PR-',Inc_X])
752         wait_ready1(S1)
753         X_pos=X_pos-str2num(Inc_X);
754         set(handles.Pos_Map_X,'String',num2str(X_pos))
755
756     end
757     Y_index=Y_index+1;
758 end
759
760     % record a spectrum at pos: (X_pos,Y_pos) now with extra
761     % debugging
762
763     if objExp.Start ( objDoc )
764         l = 0;
765         while l < maxDelay
766             statusBit = objExp.GetParam ( 'EXP_RUNNING' );
767             if statusBit == 0
768                 break;
769             end
770             pause(0.01);
771             l=l+1;
772         end
773         if l == maxDelay
774             sprintf('Maximum delay exceeded! In file %d',num2str(stepCounter));
775         end
776
777         objDoc.Close;
778     end
779
780     % Move in +Y direction by Inc_Y
781     fprintf(S1,['2PR',Inc_Y])
782     wait_ready2(S1)
783     Y_pos=Y_pos+str2num(Inc_Y);
784     set(handles.Pos_Map_Y,'String',num2str(Y_pos))
785 end
786 set(handles.Run_button,'BackgroundColor',[0.925,0.914,0.847])
787
788 else
789     errordlg('Serial port need to be open','Error');
790 end
791
792
793
794
795 % --- Wait until status S1 is ready
```

```
796 function wait_ready1(port)
797 fprintf(port, '1TS')
798 status=fscanf(port);
799 while (status(4) ≠ '0')
800     fprintf(port, '1TS');
801     status=fscanf(port);
802 end
803 %
804 % --- Wait until status S2 is ready
805 function wait_ready2(port)
806 fprintf(port, '2TS')
807 status=fscanf(port);
808 while (status(4) ≠ '0')
809     fprintf(port, '2TS');
810     status=fscanf(port);
811 end
812 %
813 % -----
814
815
816
817
818
819 % -----
820 %             Display data
821 % -----
822 %
823
824 function Edit_Path_Callback(hObject, eventdata, handles)
825
826
827
828
829
830
831
832 % --- Executes on slider movement.
833 function slider_E_Callback(hObject, eventdata, handles)
834
835 set(hObject, 'Max', handles.Max_slider);
836 set(hObject, 'SliderStep', handles.SliderStep);
837
838 %obtains the slider value from the slider component
839 handles.sliderValue = get(handles.slider_E, 'Value');
840
841 %puts the slider value into the edit text components
842 slider_ind=fix(handles.sliderValue)+1;
843
```

```

844 set(handles.WV_Value, 'String', num2str(slider_ind));
845
846 set(handles.WV, 'String', num2str(handles.wl(slider_ind)));
847
848 set(handles.axes1, 'NextPlot', 'replacechildren');
849
850 a=imagesc(handles.x,handles.y,handles.M(:,:,slider_ind));
851 set(a, 'hitest', 'off');
852
853 colorbar;
854 xlabel('steps');
855 ylabel('steps');
856
857 % Update handles structure
858 guidata(hObject, handles);
859
860
861
862
863
864 % --- Executes on button press in Display_Button.
865 function Display_Button_Callback(hObject, eventdata, handles)
866
867 % Creation Matrix Data
868 X_max=str2num(get(handles.X_max_edit, 'String'));
869 Y_max=str2num(get(handles.Y_max_edit, 'String'));
870
871 Inc_X=str2num(get(handles.Step_Size_X_edit, 'String'));
872 Inc_Y=str2num(get(handles.Step_Size_Y_edit, 'String'));
873
874 col=X_max/Inc_X+1;
875 lines=Y_max/Inc_Y+1;
876
877 file_num=col*lines;
878
879 M=zeros(lines,col,handles.pix);
880
881 k=0;
882 for i=1:lines
883     for j=1:col
884         fid = fopen ( [strcat(get(handles.Edit_Path, 'String'), '\spec_'), num2str(k), '.SPE']);
885         %fid = fopen ( 'test_1.SPE' );
886         tmp          = fread ( fid, 3263, 'int8');
887         polynom_coeff = fread ( fid,    6, 'double');
888         tmp          = fread ( fid,  789, 'int8');
889         data         = fread ( fid,      'int32' );
890         fclose (fid);
891         M(i,j,1:end)=data;

```

```
892         k=k+1;
893     end
894 end
895 % inverting each second line to respect the scan motion
896 B=M(2:2:end,:,:);
897 C=B(:,end:-1:1,:);
898 M(2:2:end,:,:)=C;
899
900 handles.M=M;
901
902 % Display map at wavelength index given by handles.sliderValue
903 handles.x = 0:Inc_X:X_max;
904 handles.y = 0:Inc_Y:Y_max;
905
906 axes(handles.axes1);
907
908 set(gca,'NextPlot','replacechildren');
909
910 a=imagesc(handles.x,handles.y,...
911     handles.M(:,:,fix(handles.sliderValue)));
912
913 colorbar
914 xlabel('steps');
915 ylabel('steps');
916
917 handles.wl = polyval ( polynom_coeff(end:-1:1) , 1:length(data) )';
918
919 dataSpec = ones(1, 512);
920
921 dataSpec = squeeze(M(20,50,:));
922
923
924
925
926 figure(1)
927 plot(handles.wl , dataSpec);
928
929 % set(handles.axes1,'hittest','off');
930 set(a,'hittest','off');
931
932 guidata(hObject , handles);
933
934
935
936 % --- Executes on mouse press over axes background.
937 function axes1_ButtonDownFcn(hObject , eventdata , handles)
938
939 location = get(handles.axes1,'CurrentPoint');
```

```

940 x = round(location(1,1))
941 y = round(location(1,2))
942
943 X_max=str2num(get(handles.X_max_edit, 'String'));
944 Y_max=str2num(get(handles.Y_max_edit, 'String'));
945
946 Inc_X=str2num(get(handles.Step_Size_X_edit, 'String'));
947 Inc_Y=str2num(get(handles.Step_Size_Y_edit, 'String'));
948
949 fileNum = y * (X_max/Inc_X+1) + x
950
951 fid = fopen ( [strcat(get(handles.Edit_Path, 'String'), '\spec_'), num2str(fileNum), '.SPE' ] );
952 tmp          = fread ( fid, 3263, 'int8' );
953 polynom_coeff = fread ( fid, 6, 'double' );
954 tmp          = fread ( fid, 789, 'int8' );
955
956 if (handle.pix == 512)
957     data          = fread ( fid, 'float' );
958 else
959     data          = fread ( fid, 'int32' );
960 end
961
962
963 fclose (fid);
964
965 %TODO
966 % inverting each second line to respect the scan motion
967
968 % scale, poly coefficients...
969
970 scrsz = get(0, 'ScreenSize');
971
972 figure('Position', [1 scrsz(4)/2 scrsz(3)/2 scrsz(4)/2])
973 plot(data);
974
975
976
977 % -----
978
979
980 % -----
981 %           Close GUI function
982 % -----
983 %
984 function closeGUI(src, evnt)
985
986 selection = questdlg('Are sure you want to close RT_setup?', ...
987                     'Close Request Function', ...

```

```

988         'Yes','No','Yes');
989 switch selection,
990     case 'Yes',
991         delete(gcf)
992
993     case 'No'
994         return
995 end
996 % -----

```

A.2 getbeam.m

```

1 % -----
2 % -----
3 %             Subroutine to automatize beam
4 %             are calculations @ Vlab
5 %
6 %             David Lakatos, November 2009, TU Delft
7 % -----
8 % -----
9
10
11
12
13 function varargout = getBeam(varargin)
14 % GETBEAM M-file for getBeam.fig
15 %     GETBEAM, by itself, creates a new GETBEAM or raises the existing
16 %     singleton*.
17 %
18 %     H = GETBEAM returns the handle to a new GETBEAM or the handle to
19 %     the existing singleton*.
20 %
21 %     GETBEAM('CALLBACK',hObject,eventData,handles,...) calls the local
22 %     function named CALLBACK in GETBEAM.M with the given input arguments.
23 %
24 %     GETBEAM('Property','Value',...) creates a new GETBEAM or raises the
25 %     existing singleton*. Starting from the left, property value pairs are
26 %     applied to the GUI before getBeam_OpeningFcn gets called. An
27 %     unrecognized property name or invalid value makes property application
28 %     stop. All inputs are passed to getBeam_OpeningFcn via varargin.
29 %
30 %     *See GUI Options on GUIDE's Tools menu. Choose "GUI allows only one
31 %     instance to run (singleton)".
32 %

```



```
33 % See also: GUIDE, GUIDATA, GUIHANDLES
34
35 % Edit the above text to modify the response to help getBeam
36
37 % Last Modified by GUIDE v2.5 14-Sep-2009 11:02:42
38
39 % Begin initialization code - DO NOT EDIT
40 gui_Singleton = 1;
41 gui_State = struct('gui_Name',       mfilename, ...
42                  'gui_Singleton',   gui_Singleton, ...
43                  'gui_OpeningFcn', @getBeam_OpeningFcn, ...
44                  'gui_OutputFcn',  @getBeam_OutputFcn, ...
45                  'gui_LayoutFcn',  [], ...
46                  'gui_Callback',   []);
47 if nargin && ischar(varargin{1})
48     gui_State.gui_Callback = str2func(varargin{1});
49 end
50
51 if nargin
52     [varargout{1:nargout}] = gui_mainfcn(gui_State, varargin{:});
53 else
54     gui_mainfcn(gui_State, varargin{:});
55 end
56 % End initialization code - DO NOT EDIT
57
58
59 % --- Executes just before getBeam is made visible.
60 function getBeam_OpeningFcn(hObject, eventdata, handles, varargin)
61 % This function has no output args, see OutputFcn.
62 % hObject    handle to figure
63 % eventdata  reserved - to be defined in a future version of MATLAB
64 % handles    structure with handles and user data (see GUIDATA)
65
66 backgroundImage = importdata('headerklimt.jpg');
67 %select the axes
68 axes(handles.axes1);
69 %place image onto the axes
70 image(backgroundImage);
71 %remove the axis tick marks
72 axis off
73
74 backgroundImage = importdata('headerklimt2.jpg');
75 %select the axes
76 axes(handles.axes2);
77 %place image onto the axes
78 image(backgroundImage);
79 %remove the axis tick marks
80 axis off
```

```
81
82
83 % Choose default command line output for getBeam
84 handles.output = hObject;
85
86 % Update handles structure
87 guidata(hObject, handles);
88
89 % UIWAIT makes getBeam wait for user response (see UIRESUME)
90 % uiwait(handles.figure1);
91
92
93 % --- Outputs from this function are returned to the command line.
94 function varargout = getBeam_OutputFcn(hObject, eventdata, handles)
95 % varargout cell array for returning output args (see VARARGOUT);
96 % hObject handle to figure
97 % eventdata reserved - to be defined in a future version of MATLAB
98 % handles structure with handles and user data (see GUIDATA)
99
100 % Get default command line output from handles structure
101 varargout{1} = handles.output;
102
103
104
105 function edit2_Callback(hObject, eventdata, handles)
106 % hObject handle to edit2 (see GCBO)
107 % eventdata reserved - to be defined in a future version of MATLAB
108 % handles structure with handles and user data (see GUIDATA)
109
110 % Hints: get(hObject,'String') returns contents of edit2 as text
111 % str2double(get(hObject,'String')) returns contents of edit2 as a double
112
113
114 % --- Executes during object creation, after setting all properties.
115 function edit2_CreateFcn(hObject, eventdata, handles)
116 % hObject handle to edit2 (see GCBO)
117 % eventdata reserved - to be defined in a future version of MATLAB
118 % handles empty - handles not created until after all CreateFcns called
119
120 % Hint: edit controls usually have a white background on Windows.
121 % See ISPC and COMPUTER.
122 if ispc && isequal(get(hObject,'BackgroundColor'), get(0,'defaultUicontrolBackgroundColor'))
123     set(hObject,'BackgroundColor','white');
124 end
125
126
127 % --- Executes on button press in viewButton.
128 function viewButton_Callback(hObject, eventdata, handles)
```

```
129 % hObject    handle to viewButton (see GCBO)
130 % eventdata  reserved - to be defined in a future version of MATLAB
131 % handles    structure with handles and user data (see GUIDATA)
132
133 figure
134 fileName = strcat('C:\Documents and Settings\localadmin\Desktop\RT_setup',...
135     get(handles.edit2,'String'));
136 a=imread(fileName);
137 b=a(:,:,1);
138 image(b);
139
140
141
142
143
144 % --- Executes on button press in radiobutton1.
145 function radiobutton1_Callback(hObject, eventdata, handles)
146 % hObject    handle to radiobutton1 (see GCBO)
147 % eventdata  reserved - to be defined in a future version of MATLAB
148 % handles    structure with handles and user data (see GUIDATA)
149
150 % Hint: get(hObject,'Value') returns toggle state of radiobutton1
151
152
153 % --- Executes on button press in radiobutton2.
154 function radiobutton2_Callback(hObject, eventdata, handles)
155 % hObject    handle to radiobutton2 (see GCBO)
156 % eventdata  reserved - to be defined in a future version of MATLAB
157 % handles    structure with handles and user data (see GUIDATA)
158
159 % Hint: get(hObject,'Value') returns toggle state of radiobutton2
160
161
162 % --- Executes on button press in pushbutton2.
163 function pushbutton2_Callback(hObject, eventdata, handles)
164 % hObject    handle to pushbutton2 (see GCBO)
165 % eventdata  reserved - to be defined in a future version of MATLAB
166 % handles    structure with handles and user data (see GUIDATA)
167 fileName = strcat('C:\Documents and Settings\localadmin\Desktop\RT_setup',...
168     get(handles.edit2,'String'));
169 a=imread(fileName);
170 b=a(:,:,1);
171
172 if get(handles.radiobutton1,'Value') == 1
173     %the X coordinate should be used
174     cut=b(:,str2num(get(handles.edit3,'String')));
175 elseif get(handles.radiobutton1,'Value') == 0
176     cut=b(str2num(get(handles.edit4,'String')),:);
```

```
177 end
178
179 figure
180 plot(cut);
181
182
183
184 function edit3_Callback(hObject, eventdata, handles)
185 % hObject    handle to edit3 (see GCBO)
186 % eventdata  reserved - to be defined in a future version of MATLAB
187 % handles    structure with handles and user data (see GUIDATA)
188
189 % Hints: get(hObject,'String') returns contents of edit3 as text
190 %        str2double(get(hObject,'String')) returns contents of edit3 as a double
191
192
193 % --- Executes during object creation, after setting all properties.
194 function edit3_CreateFcn(hObject, eventdata, handles)
195 % hObject    handle to edit3 (see GCBO)
196 % eventdata  reserved - to be defined in a future version of MATLAB
197 % handles    empty - handles not created until after all CreateFcns called
198
199 % Hint: edit controls usually have a white background on Windows.
200 %        See ISPC and COMPUTER.
201 if ispc && isequal(get(hObject,'BackgroundColor'), get(0,'defaultUicontrolBackgroundColor'))
202     set(hObject,'BackgroundColor','white');
203 end
204
205
206
207 function edit4_Callback(hObject, eventdata, handles)
208 % hObject    handle to edit4 (see GCBO)
209 % eventdata  reserved - to be defined in a future version of MATLAB
210 % handles    structure with handles and user data (see GUIDATA)
211
212 % Hints: get(hObject,'String') returns contents of edit4 as text
213 %        str2double(get(hObject,'String')) returns contents of edit4 as a double
214
215
216 % --- Executes during object creation, after setting all properties.
217 function edit4_CreateFcn(hObject, eventdata, handles)
218 % hObject    handle to edit4 (see GCBO)
219 % eventdata  reserved - to be defined in a future version of MATLAB
220 % handles    empty - handles not created until after all CreateFcns called
221
222 % Hint: edit controls usually have a white background on Windows.
223 %        See ISPC and COMPUTER.
224 if ispc && isequal(get(hObject,'BackgroundColor'), get(0,'defaultUicontrolBackgroundColor'))
```

```
225     set(hObject, 'BackgroundColor', 'white');
226 end
227
228
229
230 function edit5_Callback(hObject, eventdata, handles)
231 % hObject    handle to edit5 (see GCBO)
232 % eventdata  reserved - to be defined in a future version of MATLAB
233 % handles    structure with handles and user data (see GUIDATA)
234
235 % Hints: get(hObject, 'String') returns contents of edit5 as text
236 %         str2double(get(hObject, 'String')) returns contents of edit5 as a double
237
238
239 % --- Executes during object creation, after setting all properties.
240 function edit5_CreateFcn(hObject, eventdata, handles)
241 % hObject    handle to edit5 (see GCBO)
242 % eventdata  reserved - to be defined in a future version of MATLAB
243 % handles    empty - handles not created until after all CreateFcns called
244
245 % Hint: edit controls usually have a white background on Windows.
246 %         See ISPC and COMPUTER.
247 if ispc && isequal(get(hObject, 'BackgroundColor'), get(0, 'defaultUicontrolBackgroundColor'))
248     set(hObject, 'BackgroundColor', 'white');
249 end
250
251
252
253 function edit6_Callback(hObject, eventdata, handles)
254 % hObject    handle to edit6 (see GCBO)
255 % eventdata  reserved - to be defined in a future version of MATLAB
256 % handles    structure with handles and user data (see GUIDATA)
257
258 % Hints: get(hObject, 'String') returns contents of edit6 as text
259 %         str2double(get(hObject, 'String')) returns contents of edit6 as a double
260
261
262 % --- Executes during object creation, after setting all properties.
263 function edit6_CreateFcn(hObject, eventdata, handles)
264 % hObject    handle to edit6 (see GCBO)
265 % eventdata  reserved - to be defined in a future version of MATLAB
266 % handles    empty - handles not created until after all CreateFcns called
267
268 % Hint: edit controls usually have a white background on Windows.
269 %         See ISPC and COMPUTER.
270 if ispc && isequal(get(hObject, 'BackgroundColor'), get(0, 'defaultUicontrolBackgroundColor'));
271     set(hObject, 'BackgroundColor', 'white');
272 end
```

```

273
274
275 % --- Executes on button press in pushbutton3.
276 function pushbutton3_Callback(hObject, eventdata, handles)
277 % hObject    handle to pushbutton3 (see GCBO)
278 % eventdata  reserved - to be defined in a future version of MATLAB
279 % handles    structure with handles and user data (see GUIDATA)
280
281 diff = abs(str2num(get(handles.edit5,'String')) - str2num(get(handles.edit6,'String')));
282
283 if get(handles.radiobutton1,'Value') == 1
284     beamValue = 50/480* diff;
285
286 elseif get(handles.radiobutton1,'Value') == 0
287
288 end
289
290 %set(handles.text3,'String', num2str(beamValue));
291 set(handles.text3,'String', ['Beam size: ',num2str(beamValue),' um']);
292
293 optE = (beamValue/2)^2 * pi * 10^-2 * 4.98;
294
295 set(handles.text6,'String', ['Opt. energy: ',num2str(optE),' mW']);
296
297 handles.output = hObject;
298 guidata(hObject,handles);

```

A.3 plemap.m

```

1 % -----
2 % -----
3 %           PLE map automatisisation @ Vlab
4 %
5 %           David Lakatos, November 2009, TU Delft
6 % -----
7 % -----
8
9 function varargout = plemap(varargin)
10
11 % Begin initialization code - DO NOT EDIT
12 gui_Singleton = 1;
13 gui_State = struct('gui_Name',       mfilename, ...
14                   'gui_Singleton',   gui_Singleton, ...
15                   'gui_OpeningFcn',  @plemap_OpeningFcn, ...

```

```
16         'gui_OutputFcn', @plemap_OutputFcn, ...
17         'gui_LayoutFcn', [] , ...
18         'gui_Callback', []);
19 if nargin && ischar(varargin{1})
20     gui_State.gui_Callback = str2func(varargin{1});
21 end
22
23 if narginout
24     [varargout{1:nargout}] = gui_mainfcn(gui_State, varargin{:});
25 else
26     gui_mainfcn(gui_State, varargin{:});
27 end
28 % End initialization code - DO NOT EDIT
29
30
31 % --- Executes just before plemap is made visible.
32 function plemap_OpeningFcn(hObject, eventdata, handles, varargin)
33 global S1;
34
35 clc;
36
37 %deZIGNNN
38
39 backgroundImage = importdata('brecht.jpg');
40 %select the axes
41 axes(handles.axes2);
42 %place image onto the axes
43 image(backgroundImage);
44 %remove the axis tick marks
45 axis off
46
47 backgroundImage = importdata('brecht2.jpg');
48 %select the axes
49 axes(handles.axes3);
50 %place image onto the axes
51 image(backgroundImage);
52 %remove the axis tick marks
53 axis off
54
55 backgroundImage = importdata('brecht3.jpg');
56 %select the axes
57 axes(handles.axes4);
58 %place image onto the axes
59 image(backgroundImage);
60 %remove the axis tick marks
61 axis off
62
63 % Serial communication INIT
```

```
64
65 instrreset;
66
67 S1=serial('COM1');
68 set(S1, 'BaudRate', 115200, 'DataBits', 8, 'StopBits', 1, 'FlowControl', 'hardware');
69
70 fopen(S1);
71
72 %Motor initialisation
73
74 if not(libisloaded('USMCDLL'))
75     loadlibrary('USMCDLL','USMCDLL.h')
76 end
77
78 global Devices_st;
79 global StartParam;
80 global State;
81 global Mode;
82
83 Devices_st = libstruct('USMC_Devices_st');
84 StartParam = libstruct('USMC_StartParameters_st');
85 State = libstruct('USMC_State_st');
86 Mode = libstruct('USMC_Mode_st');
87
88 %one member of the structure has to be initilised
89 Devices_st.NOD=0;
90
91 %Init command
92 retval=calllib('USMCDLL', 'USMC_Init', Devices_st);
93
94 %Get the status
95 Number_of_devices = Devices_st.NOD;
96
97 %every struct needs one field to be initialised
98 State.FullPower=1;
99 StartParam.Sdivisor=1;
100
101 retStart=calllib('USMCDLL', 'USMC_GetStartParameters', 0, StartParam);
102 retState=calllib('USMCDLL', 'USMC_GetState', 0, State);
103
104 if (retval==0)
105     set(handles.motorStatus, 'String', 'Initialised');
106     set(handles.motorStatus, 'BackgroundColor', [0.2,0.8,0]);
107     set(handles.motorStatus, 'ForegroundColor', [1,1,1])
108
109     set(handles.temperature, 'String', [num2str(State.Temp), ' C']);
110     set(handles.motorPos, 'String', num2str(State.CurPos));
111 end
```



```
112
113 handles.output = hObject;
114 guidata(hObject, handles);
115
116
117 % --- Outputs from this function are returned to the command line.
118 function varargout = plemap_OutputFcn(hObject, eventdata, handles)
119 % varargout cell array for returning output args (see VARARGOUT);
120 % hObject handle to figure
121 % eventdata reserved - to be defined in a future version of MATLAB
122 % handles structure with handles and user data (see GUIDATA)
123
124 % Get default command line output from handles structure
125 varargout{1} = handles.output;
126
127
128
129 function from_Callback(hObject, eventdata, handles)
130 % hObject handle to from (see GCBO)
131 % eventdata reserved - to be defined in a future version of MATLAB
132 % handles structure with handles and user data (see GUIDATA)
133
134 % Hints: get(hObject,'String') returns contents of from as text
135 % str2double(get(hObject,'String')) returns contents of from as a double
136
137
138 % --- Executes during object creation, after setting all properties.
139 function from_CreateFcn(hObject, eventdata, handles)
140 % hObject handle to from (see GCBO)
141 % eventdata reserved - to be defined in a future version of MATLAB
142 % handles empty - handles not created until after all CreateFcns called
143
144 % Hint: edit controls usually have a white background on Windows.
145 % See ISPC and COMPUTER.
146 if ispc && isequal(get(hObject,'BackgroundColor'), get(0,'defaultUicontrolBackgroundColor'))
147 set(hObject,'BackgroundColor','white');
148 end
149
150
151
152 function to_Callback(hObject, eventdata, handles)
153 % hObject handle to to (see GCBO)
154 % eventdata reserved - to be defined in a future version of MATLAB
155 % handles structure with handles and user data (see GUIDATA)
156
157 % Hints: get(hObject,'String') returns contents of to as text
158 % str2double(get(hObject,'String')) returns contents of to as a double
159
```

```
160
161 % --- Executes during object creation, after setting all properties.
162 function to_CreateFcn(hObject, eventdata, handles)
163 % hObject    handle to to (see GCBO)
164 % eventdata  reserved - to be defined in a future version of MATLAB
165 % handles    empty - handles not created until after all CreateFcns called
166
167 % Hint: edit controls usually have a white background on Windows.
168 %         See ISPC and COMPUTER.
169 if ispc && isequal(get(hObject,'BackgroundColor'), get(0,'defaultUicontrolBackgroundColor'))
170     set(hObject,'BackgroundColor','white');
171 end
172
173
174
175 function intsec_Callback(hObject, eventdata, handles)
176 % hObject    handle to intsec (see GCBO)
177 % eventdata  reserved - to be defined in a future version of MATLAB
178 % handles    structure with handles and user data (see GUIDATA)
179
180 % Hints: get(hObject,'String') returns contents of intsec as text
181 %         str2double(get(hObject,'String')) returns contents of intsec as a double
182
183
184 % --- Executes during object creation, after setting all properties.
185 function intsec_CreateFcn(hObject, eventdata, handles)
186 % hObject    handle to intsec (see GCBO)
187 % eventdata  reserved - to be defined in a future version of MATLAB
188 % handles    empty - handles not created until after all CreateFcns called
189
190 % Hint: edit controls usually have a white background on Windows.
191 %         See ISPC and COMPUTER.
192 if ispc && isequal(get(hObject,'BackgroundColor'), get(0,'defaultUicontrolBackgroundColor'))
193     set(hObject,'BackgroundColor','white');
194 end
195
196
197 % --- Executes on button press in pushbutton1.
198 function pushbutton1_Callback(hObject, eventdata, handles)
199 % hObject    handle to pushbutton1 (see GCBO)
200 % eventdata  reserved - to be defined in a future version of MATLAB
201 % handles    structure with handles and user data (see GUIDATA)
202 global StartParam;
203 global State;
204 global S1;
205
206 %creating COM objects to communicate with ActiveX server
207 objExp = actxserver ( 'WinX32.ExpSetup' );
```

```

208 objDoc = actxserver ( 'WinX32.DocFile' );
209
210 %Set parameters in WInSpec
211 objExp.SetParam('EXP_FILEINCCOUNT',0);
212 objExp.SetParam('EXP_DATFILENAME','LastData');
213 % objExp.SetParam('EXP_DATFILENAME','C:\Documents and Settings\localadmin\Desktop\'. ...
214 %     ,get(handles.path,'String'));
215
216 from = str2num(get(handles.from,'String'));
217 to = str2num(get(handles.to,'String'));
218 step = str2num(get(handles.step,'String'));
219
220 Δ=abs(from-to);
221
222 cycles = (Δ/step)+1
223
224 pause(2);
225 StartParam.Sdivisor=1;
226
227 dataNorm = zeros(cycles,4);
228
229 for i=0:(cycles-1)
230
231     %moving the amount needed
232     %% for MIRA calib = 206.68
233     %% for 3900 calib = -714.28
234     calib = -714.28;
235
236     calllib('USMCDLL','USMC_Start',0,(i*round(step*calib)),40.0,StartParam);
237
238
239
240     % this corresponds to integration time * 1.5...if the
241     % experimtn has not finished we move onto the next wavelength
242     %maxDelay = 150);
243     statusBit = 1;
244
245     %wait to reach next wavelength
246     pause(3);
247
248     fprintf(S1,'%POWER?');
249     powTemp = str2num(fscanf(S1));
250
251     %normalisation file create
252     fid = fopen(['C:\Documents and Settings\localadmin\Desktop\''. ...
253         get(handles.path,'String'),'normalization.txt'], 'a');
254
255     fprintf(fid, '%f %f\r\n', ...

```

```
256         (from+i*step),powTemp);
257
258     fclose(fid);
259
260
261     dataNorm((i+1),1) = i;
262     dataNorm((i+1),2) = powTemp;
263
264     %reached wavelength, now let's record spectrum
265     if objExp.Start ( objDoc )
266         l = 0;
267         while l < 100000
268             statusBit = objExp.GetParam ( 'EXP_RUNNING' );
269             if statusBit == 0
270                 break;
271             end
272             pause(0.01);
273             l=l+1;
274         end
275         %     if l == maxDelay
276         %         sprintf('Maximum delay exceeded! In file %d',num2str(cycles));
277         %     end
278
279         objDoc.Close;
280     end
281     %updating information about the motor
282     calllib('USMCDLL', 'USMC_GetState', 0, State);
283     set(handles.temperature,'String',[num2str(State.Temp),' C']);
284     set(handles.motorPos,'String',num2str(State.CurPos));
285     set(handles.curWL,'String',num2str(from+i*step));
286 end
287
288 %DISPLAY
289
290 M=zeros(cycles,512);
291 length(M);
292 a=1;
293
294 [z,zz] = textread(...
295     ['C:\Documents and Settings\localadmin\Desktop\',...
296     get(handles.path,'String'),'normalization.txt'], ...
297     '%f %f', cycles);
298
299 A = [z,zz];
300 sortrows(A,1);
301
302 excitation = A(:,1);
303 power = A(:,2);
```

```
304
305 maxPower = max(power);
306
307 axesExcitation = sort(excitation);
308
309 for k = 0:(cycles-1)
310     fid = fopen (...
311         ['C:\Documents and Settings\localadmin\Desktop\',...
312         get(handles.path,'String'),...
313         '\LastData',num2str(k),'.SPE']);
314
315     tmp          = fread ( fid, 3263, 'int8');
316     polynom_coeff = fread ( fid,   6, 'double');
317     tmp          = fread ( fid,  789, 'int8');
318     intensity    = fread ( fid,      'float');
319
320     fclose(fid);
321
322     emission = polyval ( polynom_coeff(end:-1:1) , 1:length(intensity));
323
324     for l = 1:512
325         M(a,l) = (power(a) * intensity(l)) / maxPower;
326     end
327     a=a+1;
328 end
329
330 figure(1)
331 imagesc(emission,axesExcitation,M(:,,:));
332 title('PLE map','fontsize',12,'fontweight','b')
333 xlabel('Emission wavelength [nm]')
334 ylabel('Excitation wavelength [nm]')
335
336 %END OF DISPLAY
337
338 handles.output = hObject;
339 guidata(hObject, handles);
340
341
342 function step_Callback(hObject, eventdata, handles)
343 % hObject    handle to step (see GCBO)
344 % eventdata  reserved - to be defined in a future version of MATLAB
345 % handles    structure with handles and user data (see GUIDATA)
346
347 % Hints: get(hObject,'String') returns contents of step as text
348 %        str2double(get(hObject,'String')) returns contents of step as a double
349
350
351 % --- Executes during object creation, after setting all properties.
```

```
352 function step_CreateFcn(hObject, eventdata, handles)
353 % hObject    handle to step (see GCBO)
354 % eventdata  reserved - to be defined in a future version of MATLAB
355 % handles    empty - handles not created until after all CreateFcns called
356
357 % Hint: edit controls usually have a white background on Windows.
358 %         See ISPC and COMPUTER.
359 if ispc && isequal(get(hObject,'BackgroundColor'), get(0,'defaultUicontrolBackgroundColor'))
360     set(hObject,'BackgroundColor','white');
361 end
362
363
364 % --- If Enable == 'on', executes on mouse press in 5 pixel border.
365 % --- Otherwise, executes on mouse press in 5 pixel border or over motorStatus.
366 function motorStatus_ButtonDownFcn(hObject, eventdata, handles)
367 % hObject    handle to motorStatus (see GCBO)
368 % eventdata  reserved - to be defined in a future version of MATLAB
369 % handles    structure with handles and user data (see GUIDATA)
370
371
372
373 function setPos_Callback(hObject, eventdata, handles)
374 % hObject    handle to setPos (see GCBO)
375 % eventdata  reserved - to be defined in a future version of MATLAB
376 % handles    structure with handles and user data (see GUIDATA)
377
378 % Hints: get(hObject,'String') returns contents of setPos as text
379 %         str2double(get(hObject,'String')) returns contents of setPos as a double
380
381
382 % --- Executes during object creation, after setting all properties.
383 function setPos_CreateFcn(hObject, eventdata, handles)
384 % hObject    handle to setPos (see GCBO)
385 % eventdata  reserved - to be defined in a future version of MATLAB
386 % handles    empty - handles not created until after all CreateFcns called
387
388 % Hint: edit controls usually have a white background on Windows.
389 %         See ISPC and COMPUTER.
390 if ispc && isequal(get(hObject,'BackgroundColor'), get(0,'defaultUicontrolBackgroundColor'))
391     set(hObject,'BackgroundColor','white');
392 end
393
394
395 % --- Executes on button press in pushbutton2.
396 function pushbutton2_Callback(hObject, eventdata, handles)
397 % hObject    handle to pushbutton2 (see GCBO)
398 % eventdata  reserved - to be defined in a future version of MATLAB
399 % handles    structure with handles and user data (see GUIDATA)
```

```
400 global StartParam
401 global State
402
403 calllib('USMCDLL','USMC_SetCurrentPosition',0,str2num...
404     (get(handles.setPos,'String')));
405
406 calllib('USMCDLL','USMC_GetState',0,State);
407
408 set(handles.temperature,'String',[num2str(State.Temp),' C']);
409 set(handles.motorPos,'String',num2str(State.CurPos));
410
411
412 handles.output = hObject;
413 guidata(hObject, handles);
414
415
416
417 function moveEdit_Callback(hObject, eventdata, handles)
418 % hObject    handle to moveEdit (see GCBO)
419 % eventdata  reserved - to be defined in a future version of MATLAB
420 % handles    structure with handles and user data (see GUIDATA)
421
422 % Hints: get(hObject,'String') returns contents of moveEdit as text
423 %         str2double(get(hObject,'String')) returns contents of moveEdit as a double
424
425
426 % --- Executes during object creation, after setting all properties.
427 function moveEdit_CreateFcn(hObject, eventdata, handles)
428 % hObject    handle to moveEdit (see GCBO)
429 % eventdata  reserved - to be defined in a future version of MATLAB
430 % handles    empty - handles not created until after all CreateFcns called
431
432 % Hint: edit controls usually have a white background on Windows.
433 %         See ISPC and COMPUTER.
434 if ispc && isequal(get(hObject,'BackgroundColor'), get(0,'defaultUicontrolBackgroundColor'))
435     set(hObject,'BackgroundColor','white');
436 end
437
438
439 % --- Executes on button press in moveSet.
440 function moveSet_Callback(hObject, eventdata, handles)
441 % hObject    handle to moveSet (see GCBO)
442 % eventdata  reserved - to be defined in a future version of MATLAB
443 % handles    structure with handles and user data (see GUIDATA)
444 global State
445 global StartParam
446
447
```

```

448 %if the Wl has been set we can move
449 if(strcmp(get(handles.curWL,'String'),'?'))
450 else
451     to=str2num(get(handles.moveEdit,'String'));
452     from=str2num(get(handles.curWL,'String'));
453     Δ=to-from;
454
455     calllib('USMCDLL','USMC_GetState',0,State);
456     curPos=State.CurPos;
457
458     %% for MIRA calib = 206.68
459     %% for 3900 calib = -714.28
460     calib = -714.28;
461
462     steps2move = round(Δ * calib);
463     StartParam.Sdivisor=1;
464
465     calllib('USMCDLL','USMC_Start',0,(curPos+steps2move),40.0,StartParam);
466     set(handles.curWL,'String',num2str(to));
467 end
468
469 handles.output = hObject;
470 guidata(hObject, handles);
471
472
473 function setWL_Callback(hObject, eventdata, handles)
474 % hObject     handle to setWL (see GCBO)
475 % eventdata   reserved - to be defined in a future version of MATLAB
476 % handles     structure with handles and user data (see GUIDATA)
477
478 % Hints: get(hObject,'String') returns contents of setWL as text
479 %         str2double(get(hObject,'String')) returns contents of setWL as a double
480
481
482 % --- Executes during object creation, after setting all properties.
483 function setWL_CreateFcn(hObject, eventdata, handles)
484 % hObject     handle to setWL (see GCBO)
485 % eventdata   reserved - to be defined in a future version of MATLAB
486 % handles     empty - handles not created until after all CreateFcns called
487
488 % Hint: edit controls usually have a white background on Windows.
489 %         See ISPC and COMPUTER.
490 if ispc && isequal(get(hObject,'BackgroundColor'), get(0,'defaultUicontrolBackgroundColor'))
491     set(hObject,'BackgroundColor','white');
492 end
493
494
495 % --- Executes on button press in pushbutton3.

```



```
496 function pushbutton3_Callback(hObject, eventdata, handles)
497 % hObject      handle to pushbutton3 (see GCBO)
498 % eventdata    reserved - to be defined in a future version of MATLAB
499 % handles      structure with handles and user data (see GUIDATA)
500
501 temp = str2num(get(handles.setWL, 'String'));
502 set(handles.curWL, 'String', num2str(temp));
503
504
505 function pathNorm_Callback(hObject, eventdata, handles)
506 % hObject      handle to pathNorm (see GCBO)
507 % eventdata    reserved - to be defined in a future version of MATLAB
508 % handles      structure with handles and user data (see GUIDATA)
509
510 % Hints: get(hObject, 'String') returns contents of pathNorm as text
511 %          str2double(get(hObject, 'String')) returns contents of pathNorm as a double
512
513
514 % --- Executes during object creation, after setting all properties.
515 function pathNorm_CreateFcn(hObject, eventdata, handles)
516 % hObject      handle to pathNorm (see GCBO)
517 % eventdata    reserved - to be defined in a future version of MATLAB
518 % handles      empty - handles not created until after all CreateFcns called
519
520 % Hint: edit controls usually have a white background on Windows.
521 %          See ISPC and COMPUTER.
522 if ispc && isequal(get(hObject, 'BackgroundColor'), get(0, 'defaultUicontrolBackgroundColor'))
523     set(hObject, 'BackgroundColor', 'white');
524 end
525
526
527
528 function path_Callback(hObject, eventdata, handles)
529 % hObject      handle to path (see GCBO)
530 % eventdata    reserved - to be defined in a future version of MATLAB
531 % handles      structure with handles and user data (see GUIDATA)
532
533 % Hints: get(hObject, 'String') returns contents of path as text
534 %          str2double(get(hObject, 'String')) returns contents of path as a double
535
536
537 % --- Executes during object creation, after setting all properties.
538 function path_CreateFcn(hObject, eventdata, handles)
539 % hObject      handle to path (see GCBO)
540 % eventdata    reserved - to be defined in a future version of MATLAB
541 % handles      empty - handles not created until after all CreateFcns called
542
543 % Hint: edit controls usually have a white background on Windows.
```

```
544 %           See ISPC and COMPUTER.
545 if ispc && isequal(get(hObject,'BackgroundColor'), get(0,'defaultUicontrolBackgroundColor'))
546     set(hObject,'BackgroundColor','white');
547 end
```

Appendix B

Graphical User Interfaces

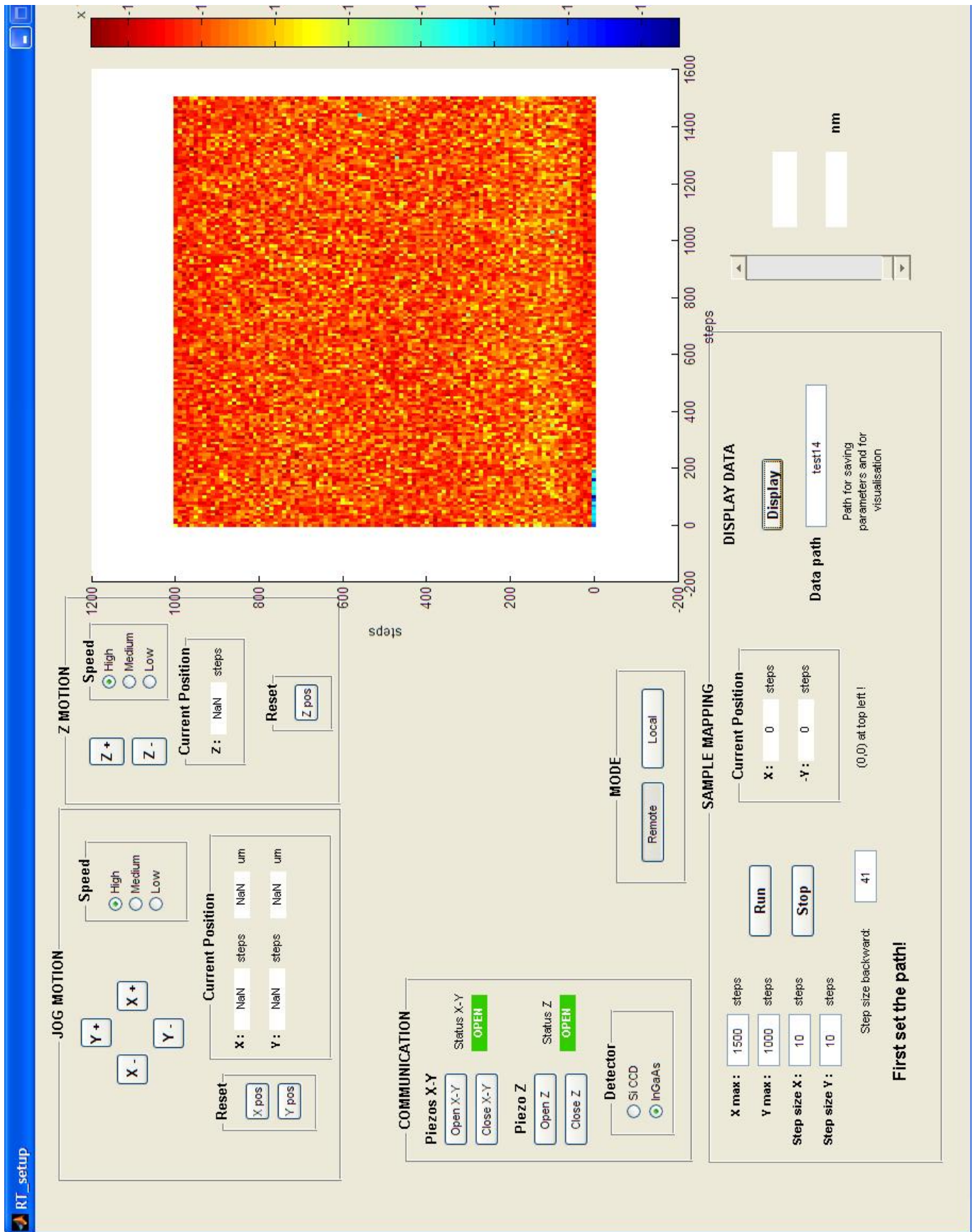


FIGURE B.1: GUI for the sample mapping automatization and stage control



FIGURE B.2: GUI for the beam area calculation

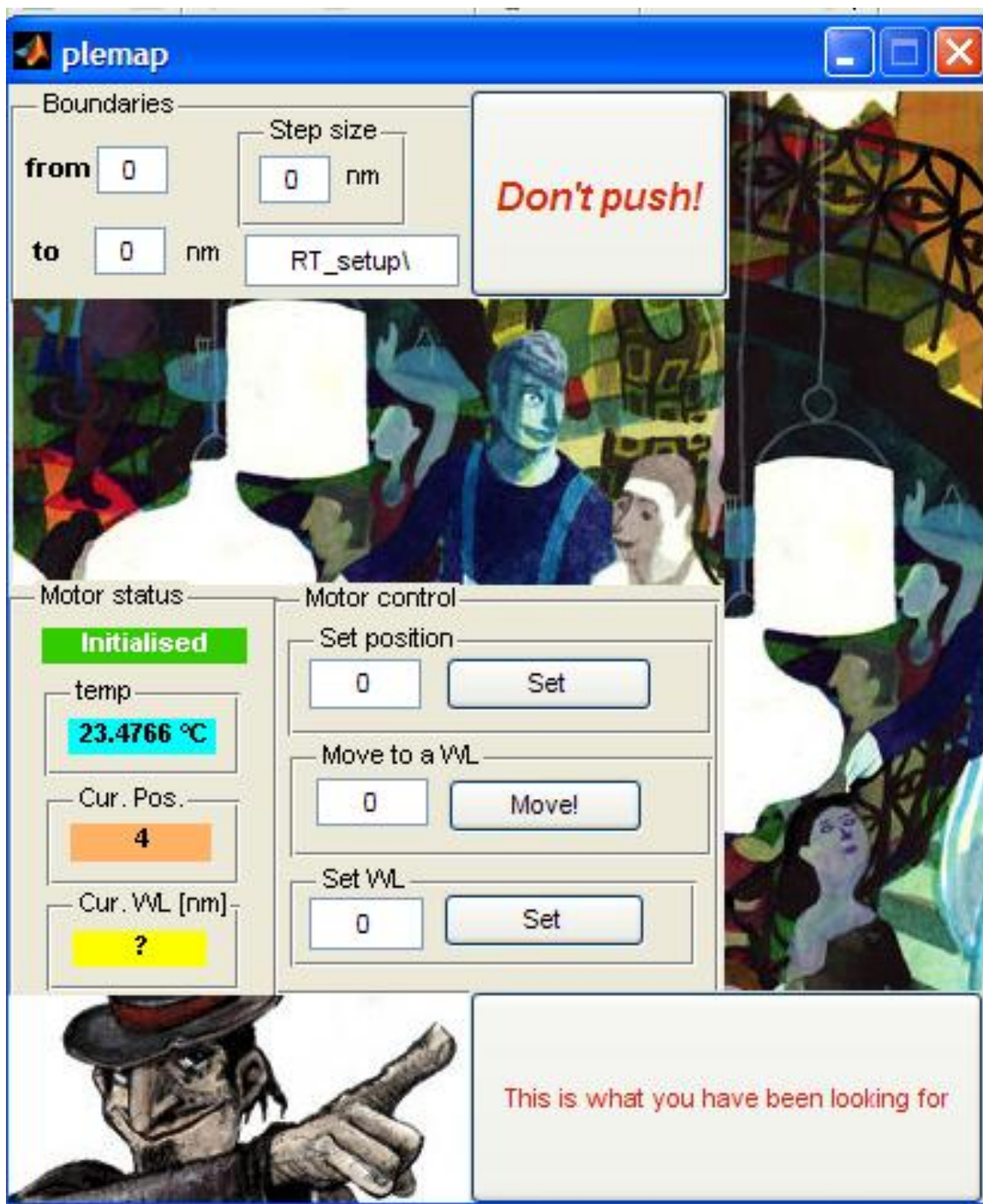


FIGURE B.3: GUI for the PLE mapping automatization

Appendix C

Table for assigning chiral indices

λ_{11} (nm)	λ_{22} (nm)	$h\nu_{11}$ (eV)	$h\nu_{22}$ (eV)	Assignment
833	483	1.488	2.567	(5,4)
873	581	1.420	2.134	(6,4)
912	693	1.359	1.789	(9,1)
952	663	1.302	1.870	(8,3)
975	567	1.272	2.187	(6,5)
1023	644	1.212	1.925	(7,5)
1053	734	1.177	1.689	(10,2)
1101	720	1.126	1.722	(9,4)
1113	587	1.114	2.112	(8,4)
1122	647	1.105	1.916	(7,6)
1139	551	1.088	2.250	(9,2)
1171	797	1.059	1.556	(12,1)
1172	716	1.058	1.732	(8,6)
1197	792	1.036	1.565	(11,3)
1244	671	0.997	1.848	(9,5)
1250	633	0.992	1.959	(10,3)
1250	786	0.992	1.577	(10,5)
1263	611	0.982	2.029	(11,1)
1267	728	0.979	1.703	(8,7)
1307	859	0.949	1.443	(13,2)
1323	790	0.937	1.569	(9,7)
1342	857	0.924	1.447	(12,4)
1372	714	0.904	1.736	(11,4)
1376	685	0.901	1.810	(12,2)
1380	756	0.898	1.640	(10,6)
1397	858	0.887	1.445	(11,6)
1414	809	0.877	1.533	(9,8)
1425	927	0.870	1.337	(15,1)
1474	868	0.841	1.428	(10,8)
1485	928	0.835	1.336	(13,5)
1496	795	0.829	1.559	(12,5)
1497	760	0.828	1.631	(13,3)
1555	892	0.797	1.390	(10,9)

FIGURE C.1: Table for assigning chiral indices to nanotubes based on their E_{11} and E_{22} energies

Bibliography

- [1] Sumio Iijima. Synthesis of carbon nanotubes. *Nature*, 354:56–58, 1991.
- [2] Marcus Freitag Phaedon Avouris and Vasili Perebeinos. Carbon-nanotube photonics and optoelectronics. *Nature Photonics* 2, 341 - 350, 2008.
- [3] M Winger A Imamoglu A Hgele, C Galland. Photon antibunching in the photoluminescence spectra of a single carbon nanotube. *Physical review letters*, 2008.
- [4] A Imamoglu C Galland. All-optical manipulation of electron spins in carbon-nanotube quantum dots. *Physical review letters*, 2008.
- [5] X. Blase. J.-C. Charlier and S. Roche. Electronic and transport properties of nanotubes. *Rev. Mod. Phys.* 79, 677, 2007.
- [6] S. K. Doorn X. Z. Liao Y. H. Zhao E. A. Akhador M. A. Hoofbauer B. J. Roop Q. X. Jia R. C. Dye D. E. Peterson S. M. Huang J. Liu L. X. Zheng, M. J. OConell and Y. T. Zhu. Ultralong single-wall carbon nanotubes. *Nature Materials* 3,673-676, 2004.
- [7] Rodney S. Ruoff and Donald C. Lorents. Mechanical and thermal properties of carbon nanotubes. *Elsevier Science*, 1995.
- [8] E Lass B Wei PM Ajayan A Modi, N Koratkar. Miniaturized gas ionization sensors using carbon nanotubes. *Nature*, 2005.
- [9] Q Wang M Lundstrom H Dai A Javey, J Guo. Ballistic carbon nanotube field-effect transistors. *Letters to Nature*, 1999.
- [10] J. P. Lu. Elastic properties of carbon nanotubes and nanoropes. *Physical Rev. Lett.*, 1997.
- [11] J. Maultzsch S. Reich and C. Thomsen. Tight-binding description of graphene. *Phys. Rev. B* 66, 035412, 2002.

- [12] G. Dresselhaus M. S. Dresselhaus and A. Jorio. Unusual properties and structure of carbon nanotube. *Annu. Rev. Mater.*, 34:247, 2004.
- [13] Chad B. Huffman Valerie C. Moore Michael S. Strano Erik H. Haroz Kristy L. Rialon Peter J. Boul William H. Noon Carter Kittrell Jianpeng Ma Robert H. Hauge R. Bruce Weisman Richard E. Smalley Michael J. O'Connell, Sergei M. Bachilo. Band gap fluorescence from individual single-walled carbon nanotubes. *Science*, Vol. 297. no. 5581, pp. 593 - 596, 2002.
- [14] Strano M S et al. Reversible, band-gap-selective protonation of single-walled carbon nanotubes in solution. *J. Phys. Chem. B* 107 697985, 2003.
- [15] Kiowski O Hennrich F Arnold K, Lebedkin S and Kappes. Matrix-imposed stress-induced shifts in the photoluminescence of single-walled carbon nanotubes at low temperatures. *Nano Lett.* 4 234954, 2004.
- [16] Murakami Y Kishimoto S Maruyama S Ohno Y, Iwasaki S and Mizutani T. Excitonic transition energies in single-walled carbon nanotubes: dependence on environmental dielectric constant. *E Phys. Status Solidi b*, 244 40025, 2007.
- [17] Homma Y Lefebvre J and Finnie. Bright band gap photoluminescence from unprocessed single-walled carbon nanotubes. *Phys. Rev. Lett.* 90 217401, 2003.
- [18] Homma Y Lefebvre J, Fraser J M and Finnie. Photoluminescence from single-walled carbon nanotubes: a comparison between suspended and micelle-encapsulated nanotubes. *Appl. Phys. A* 78 110710, 2004.
- [19] Louis E. Brus Tony F. Heinz Feng Wang, Gordana Dukovic. The optical resonances in carbon nanotubes arise from excitons. *Science*, Vol. 308. no. 5723, pp. 838 - 841, 2005.
- [20] Yoshihiro Kobayashi Yoshikazu Homma and Toshio Ogino. Growth of suspended carbon nanotube networks on 100-nm-scale silicon pillars. *APPLIED PHYSICS LETTERS*, VOLUME 81, NUMBER 12:2261-62, 2002.
- [21] Ogino T Homma Y, Kobayashi Y and Yamashita T. Growth of suspended carbon nanotube networks on 100-nm-scale silicon pillars. *Appl. Phys. Lett.* 81 22613, 2002.
- [22] Shohei Chiashi Yoshikazu Homma and Yoshihiro Kobayashi. Suspended single-wall carbon nanotubes: synthesis and optical properties. *REPORTS ON PROGRESS IN PHYSICS*, 2009.

-
- [23] Suzuki S and Kobayashi Y. Healing of low-energy irradiation-induced defects in single-walled carbon nanotubes at room temperature. *J. Phys. Chem. C* 111 45248, 2007.
- [24] <http://www.princetoninstruments.com/products/speccam/spec10>.
- [25] D. Mann et al. Electrically driven thermal light emission from individual single-walled carbon nanotubes. *Nature Nanotech* 2, 33, 2007.
- [26] O. N. Torrens et al. Photoluminescence from intertube carrier migration in single-walled carbon nanotube bundles. *Nanolett.* 6, 2864, 2006.
- [27] J. Lefebvre et al. *Phys. Rev. B* 69, 075403, 2004.
- [28] M. W. B. Wilson. Investigations into the optical properties of individual, air-suspended, single-walled carbon nanotubes. *Master thesis, Queen's University, Kingston, Canada*, 2008.
- [29] K. Kaminska et al. Real-time global raman imaging and optical manipulation of suspended carbon nanotubes. *Phys. Rev. B* 73, 235410, 2006.
- [30] Carter Kittrell Robert H. Hauge Richard E. Smalley R. Bruce Weisman Sergei M. Bachilo, Michael S. Strano. Structure-assigned optical spectra of single-walled carbon nanotubes. *Science*, Vol. 298. no. 5602, pp. 2361 - 2366, 2005.
- [31] G. A. Steele et al. Tunable few-electron double quantum dots and klein tunnelling in ultra-clean carbon nanotubes. *Nature Nanotechnology* 4, 363 - 367, 2009.

Acknowledgements

First of all I would like to thank my supervisors dr. Gilles Buchs and András Reichardt, without them this thesis would not have been possible.

Gilles, thank you for the countless hours spent in the lab and in front of the whiteboard squeezing physics into an engineer's mind and also for your patience while you were educating me.

András köszönöm mindazt a támogatást amit az évek során kaptam tőled, mind a TDK dolgozatom, mind a szakdolgozat készítése közben.

I would like to thank Leo Kouwenhoven and Val Zwiller for accepting me to the group and for providing guidance and helpful feedback on my work.

I also would like to acknowledge other people who helped me during my work. A not complete list of them: Martin, Martin, Reinier, Ilse and Benny from Delft, Zsolt and Gábor from BME and Ildikó Varga from the Erasmus Office in Budapest, who made it possible for me to spend 5 months in Delft.

I would also like to acknowledge nicotine, caffeine and alcohol as essential supporters of my thesis work.